

Modulus τ linking leptonic CP violation to baryon asymmetry in A_4 modular invariant flavor model

Hiroshi Okada ^{a,b*}, Yusuke Shimizu ^{c,d†}, Morimitsu Tanimoto ^{e‡}
and Takahiro Yoshida ^{e§}

^a*Asia Pacific Center for Theoretical Physics, Pohang 37673, Republic of Korea*

^b*Department of Physics, Pohang University of Science and Technology, Pohang 37673, Republic of Korea*

^c*Physics Program, Graduate School of Advanced Science and Engineering, Hiroshima University, Higashi-Hiroshima 739-8526, Japan*

^d*Core of Research for the Energetic Universe, Hiroshima University, Higashi-Hiroshima 739-8526, Japan*

^e*Department of Physics, Niigata University, Niigata 950-2181, Japan*

Abstract

We propose an A_4 modular invariant flavor model of leptons, in which both CP and modular symmetries are broken spontaneously by the vacuum expectation value of the modulus τ . The value of the modulus τ is restricted by the observed lepton mixing angles and lepton masses for the normal hierarchy of neutrino masses. The predictive Dirac CP phase δ_{CP} is in the ranges $[0^\circ, 50^\circ]$, $[170^\circ, 175^\circ]$ and $[280^\circ, 360^\circ]$ for $\text{Re}[\tau] < 0$, and $[0^\circ, 80^\circ]$, $[185^\circ, 190^\circ]$ and $[310^\circ, 360^\circ]$ for $\text{Re}[\tau] > 0$. The sum of three neutrino masses is predicted in $[60, 84]$ meV, and the effective mass for the $0\nu\beta\beta$ decay is in $[0.003, 3]$ meV. The modulus τ links the Dirac CP phase to the cosmological baryon asymmetry (BAU) via the leptogenesis. Due to the strong wash-out effect, the predictive baryon asymmetry Y_B can be at most the same order of the observed value. Then, the lightest right-handed neutrino mass is restricted in the range of $M_1 = [1.5, 6.5] \times 10^{13}$ GeV. We find the correlation between the predictive Y_B and the Dirac CP phase δ_{CP} . Only two predictive δ_{CP} ranges, $[5^\circ, 40^\circ]$ ($\text{Re}[\tau] > 0$) and $[320^\circ, 355^\circ]$ ($\text{Re}[\tau] < 0$) are consistent with the BAU.

*E-mail address: hiroshi.okada@apctp.org

†E-mail address: yu-shimizu@hiroshima-u.ac.jp

‡E-mail address: tanimoto@muse.sc.niigata-u.ac.jp

§E-mail address: yoshida@muse.sc.niigata-u.ac.jp

1 Introduction

One interesting approach to the origin of flavor structure is to impose a flavor symmetry on a theory. The non-Abelian discrete groups are attractive ones to understand flavor structure of quarks and leptons. The S_3 flavor symmetry was studied to understand the large mixing angle [1] in the oscillation of atmospheric neutrinos [2] as well as discussing the Cabibbo angle [3, 4]. For the last twenty years, the non-Abelian discrete symmetries of flavors have been developed [5–14], that is motivated by the precise observation of flavor mixing angles of leptons. Among them, the A_4 flavor symmetry provides a simple explanation of the existence of three families of quarks and leptons [15–21]. However, it is difficult to obtain clear clues of the A_4 flavor symmetry because of a lot of free parameters associated with scalar flavon fields.

An interesting approach to the lepton flavor problem has been put forward based on the invariance under the modular transformation [22], where the model of the finite modular group $\Gamma_3 \simeq A_4$ has been presented. In this approach, fermion matrices are written in terms of modular forms which are holomorphic functions of the modulus τ . This work inspired further studies of the modular invariance approach to the lepton flavor problem.

The finite groups S_3 , A_4 , S_4 , and A_5 are realized in modular groups [23]. Modular invariant flavor models have been also proposed on the $\Gamma_2 \simeq S_3$ [24], $\Gamma_4 \simeq S_4$ [25] and $\Gamma_5 \simeq A_5$ [26]. Phenomenological studies of the lepton flavors have been done based on A_4 [27–29], S_4 [30–32] and A_5 [33]. A clear prediction of the neutrino mixing angles and the Dirac CP phase was given in the simple lepton mass matrices with the A_4 modular symmetry [28]. The Double Covering groups T' [34, 35] and S'_4 [36, 37] were also realized in the modular symmetry. Furthermore, phenomenological studies have been developed in many works [38–88] while theoretical investigations have been also proceeded [89–106].

In order to test the flavor symmetry, the prediction of the Dirac CP phase is important. The CP transformation is non-trivial if the non-Abelian discrete flavor symmetry is set in the Yukawa sector of a Lagrangian. Then, we should discuss so-called the generalized CP symmetry in the flavor space [107–112]. The modular invariance has been also studied in the framework of the generalized CP symmetry [113, 114]. It provided a significant scheme to predict Dirac and Majorana CP phases of leptons. A viable lepton model was proposed in the modular A_4 symmetry [80], in which the CP violation is realized by fixing τ , that is, the breaking of the modular symmetry. Afterward, the systematic search of the viable A_4 model was done [81].

The CP violation by the modulus τ raises a question. Is the leptonic CP violation linked to the baryon asymmetry of the universe (BAU)? The BAU is now measured very precisely by the cosmic microwave background radiation [115]. One of the most studied scenarios for baryogenesis is the canonical leptogenesis scenario [116], in which the decays of right-handed neutrinos can generate the lepton asymmetry that is partially converted into the baryon asymmetry via the sphaleron process [117]. The sign of the BAU is controlled by the CP violation pattern in the leptonic sector. In general, the sign of the BAU cannot be predicted uniquely even if the Dirac and Majorana CP phases are determined. This is because there exist additional phases associated with right-handed neutrinos which decouple from the low energy phenomena if right-handed neutrinos are sufficiently heavy. However, there are non-trivial relations between the properties of right-handed neutrinos and the low energy observables of neutrinos in the A_4 modular symmetry. Indeed, the modulus τ controls the CP phases of both the left-handed sector of neutrinos and the right-handed one in our scheme. Under these situations, it is interesting to investigate the sign and magnitude of the BAU.

In the framework of the modular symmetry, the BAU has been studied in A_4 model of leptons,

where the source of CP violation is a complex parameter in the Dirac neutrino mass matrix in addition to the modulus τ [40]. In our work, the origin of the CP violation is only in modulus τ , therefore, it is also only the source of the leptogenesis. We present a modular A_4 invariant model with the CP symmetry, where both CP and modular symmetries are broken spontaneously by the vacuum expectation value (VEV) of the modulus τ . We discuss the phenomenological implication of this model, that is the Pontecorvo-Maki-Nakagawa-Sakata (PMNS) mixing angles [118, 119] and the Dirac CP phase of leptons, which is expected to be observed at T2K and NO ν A experiments [120, 121]. Then, we examine a link between the predictive Dirac CP phase and the BAU.

The paper is organized as follows. In section 2, we give a brief review on the CP transformation in the modular symmetry. In section 3, we present the CP invariant lepton mass matrix in the A_4 modular symmetry. In section 4, we show the phenomenological implication of lepton mixing and CP phases. In section 5, we give the framework of the leptogenesis in our model. In section 6, we discuss the link between the predictive Dirac CP phase and BAU numerically. Section 7 is devoted to the summary. In Appendices A and B, we give the tensor product of the A_4 group and the modular forms, respectively. In Appendix C, we show the definition of PMNS matrix elements and how to obtain the Dirac CP phase, the Majorana phases and the effective mass of the $0\nu\beta\beta$ decay. In Appendix D, alternative A_4 models and their results are presented. In Appendix E, we give the relevant formulae of the leptogenesis explicitly.

2 CP transformation in modular symmetry

2.1 Generalized CP symmetry

The CP transformation is non-trivial if the non-Abelian discrete flavor symmetry G is set in the Yukawa sector of a Lagrangian [112, 122]. Let us consider the chiral superfields. The CP is a discrete symmetry which involves both Hermitian conjugation of a chiral superfield $\psi(x)$ and inversion of spatial coordinates,

$$\psi(x) \rightarrow \mathbf{X}_{\mathbf{r}} \bar{\psi}(x_P) , \quad (1)$$

where $x_P = (t, -\mathbf{x})$ and $\mathbf{X}_{\mathbf{r}}$ is a unitary transformation of $\psi(x)$ in the irreducible representation \mathbf{r} of the discrete flavor symmetry G . This transformation is so-called the generalized CP transformation. If $\mathbf{X}_{\mathbf{r}}$ is the unit matrix, the CP transformation is the trivial one. This is the case for the continuous flavor symmetry [122]. However, in the framework of the non-Abelian discrete family symmetry, non-trivial choices of $\mathbf{X}_{\mathbf{r}}$ are possible. The unbroken CP transformations of $\mathbf{X}_{\mathbf{r}}$ form the group H_{CP} . Then, $\mathbf{X}_{\mathbf{r}}$ must be consistent with the flavor symmetry transformation,

$$\psi(x) \rightarrow \rho_{\mathbf{r}}(g)\psi(x) , \quad g \in G , \quad (2)$$

where $\rho_{\mathbf{r}}(g)$ is the representation matrix for g in the irreducible representation \mathbf{r} .

The consistent condition is obtained as follows. At first, perform a CP transformation $\psi(x) \rightarrow \mathbf{X}_{\mathbf{r}} \bar{\psi}(x_P)$, then apply a flavor symmetry transformation, $\bar{\psi}(x_P) \rightarrow \rho_{\mathbf{r}}^*(g) \bar{\psi}(x_P)$, and finally perform an inverse CP transformation. The whole transformation is written as $\psi(x) \rightarrow \mathbf{X}_{\mathbf{r}} \rho^*(g) \mathbf{X}_{\mathbf{r}}^{-1} \psi(x)$, which must be equivalent to some flavor symmetry $\psi(x) \rightarrow \rho_{\mathbf{r}}(g') \psi(x)$. Thus, one obtains [123]

$$\mathbf{X}_{\mathbf{r}} \rho_{\mathbf{r}}^*(g) \mathbf{X}_{\mathbf{r}}^{-1} = \rho_{\mathbf{r}}(g') , \quad g, g' \in G . \quad (3)$$

This equation defines the consistency condition, which has to be respected for consistent implementation of a generalized CP symmetry along with a flavor symmetry [124, 125].

It has been also shown that the full symmetry group is isomorphic to a semi-direct product of G and H_{CP} , that is $G \rtimes H_{CP}$, where $H_{CP} \simeq \mathbb{Z}_2^{CP}$ is the group generated by the generalised CP transformation under the assumption of \mathbf{X}_r being a symmetric matrix [125].

2.2 Modular symmetry

The modular group $\bar{\Gamma}$ is the group of linear fractional transformations γ acting on the modulus τ , belonging to the upper-half complex plane as:

$$\tau \longrightarrow \gamma\tau = \frac{a\tau + b}{c\tau + d}, \quad \text{where } a, b, c, d \in \mathbb{Z} \text{ and } ad - bc = 1, \quad \text{Im}[\tau] > 0, \quad (4)$$

which is isomorphic to $PSL(2, \mathbb{Z}) = SL(2, \mathbb{Z})/\{I, -I\}$ transformation. This modular transformation is generated by S and T ,

$$S : \tau \longrightarrow -\frac{1}{\tau}, \quad T : \tau \longrightarrow \tau + 1, \quad (5)$$

which satisfy the following algebraic relations,

$$S^2 = \mathbb{1}, \quad (ST)^3 = \mathbb{1}. \quad (6)$$

We introduce the series of groups $\Gamma(N)$, called principal congruence subgroups, where N is the level $1, 2, 3, \dots$. These groups are defined by

$$\Gamma(N) = \left\{ \begin{pmatrix} a & b \\ c & d \end{pmatrix} \in SL(2, \mathbb{Z}), \quad \begin{pmatrix} a & b \\ c & d \end{pmatrix} = \begin{pmatrix} 1 & 0 \\ 0 & 1 \end{pmatrix} \pmod{N} \right\}. \quad (7)$$

For $N = 2$, we define $\bar{\Gamma}(2) \equiv \Gamma(2)/\{I, -I\}$. Since the element $-I$ does not belong to $\Gamma(N)$ for $N > 2$, we have $\bar{\Gamma}(N) = \Gamma(N)$. The quotient groups defined as $\Gamma_N \equiv \bar{\Gamma}/\bar{\Gamma}(N)$ are finite modular groups. In these finite groups Γ_N , $T^N = \mathbb{1}$ is imposed. The groups Γ_N with $N = 2, 3, 4, 5$ are isomorphic to S_3 , A_4 , S_4 and A_5 , respectively [23].

Modular forms $f_i(\tau)$ of weight k are the holomorphic functions of τ and transform as

$$f_i(\tau) \longrightarrow (c\tau + d)^k \rho(\gamma)_{ij} f_j(\tau), \quad \gamma \in G, \quad (8)$$

under the modular symmetry, where $\rho(\gamma)_{ij}$ is a unitary matrix under Γ_N .

Under the modular transformation of Eq. (4), chiral superfields ψ_i (i denotes flavors) with weight $-k$ transform as [126],

$$\psi_i \longrightarrow (c\tau + d)^{-k} \rho(\gamma)_{ij} \psi_j. \quad (9)$$

We study global supersymmetric models, e.g., minimal supersymmetric extensions of the Standard Model (MSSM). The superpotential which is built from matter fields and modular forms is assumed to be modular invariant, i.e., to have a vanishing modular weight. For given modular forms this can be achieved by assigning appropriate weights to the matter superfields.

The kinetic terms are derived from a Kähler potential. The Kähler potential of chiral matter fields ψ_i with the modular weight $-k$ is given simply by

$$K^{\text{matter}} = \frac{1}{[i(\bar{\tau} - \tau)]^k} \sum_i |\psi_i|^2, \quad (10)$$

where the superfield and its scalar component are denoted by the same letter, and $\bar{\tau} = \tau^*$ after taking VEV of τ . The canonical form of the kinetic terms is obtained by changing the normalization of parameters [28]. The general Kähler potential consistent with the modular symmetry possibly contains additional terms [127]. However, we consider only the simplest form of the Kähler potential.

For $\Gamma_3 \simeq A_4$, the dimension of the linear space $\mathcal{M}_k(\Gamma(3))$ of modular forms of weight k is $k + 1$ [128–130], i.e., there are three linearly independent modular forms of the lowest non-trivial weight 2, which form a triplet of the A_4 group, $Y_3^{(2)}(\tau) = (Y_1(\tau), Y_2(\tau), Y_3(\tau))^T$. These modular forms have been explicitly given [22] in the symmetric base of the A_4 generators S and T for the triplet representation (see Appendix A) in Appendix B.

2.3 CP transformation of the modulus τ

The CP transformation in the modular symmetry was given by using the generalized CP symmetry [113]. We summarize the discussion in Ref. [113] briefly. Consider the CP and modular transformation γ of the chiral superfield $\psi(x)$ with weight $-k$ assigned to an irreducible unitary representation \mathbf{r} of Γ_N . The chain $CP \rightarrow \gamma \rightarrow CP^{-1} = \gamma' \in \bar{\Gamma}$ is expressed as:

$$\begin{aligned} \psi(x) &\xrightarrow{CP} \mathbf{X}_{\mathbf{r}} \bar{\psi}(x_P) \xrightarrow{\gamma} (c\tau^* + d)^{-k} \mathbf{X}_{\mathbf{r}} \rho_{\mathbf{r}}^*(\gamma) \bar{\psi}(x_P) \\ &\xrightarrow{CP^{-1}} (c\tau_{CP^{-1}}^* + d)^{-k} \mathbf{X}_{\mathbf{r}} \rho_{\mathbf{r}}^*(\gamma) \mathbf{X}_{\mathbf{r}}^{-1} \psi(x), \end{aligned} \quad (11)$$

where $\tau_{CP^{-1}}$ is the operation of CP^{-1} on τ . The result of this chain transformation should be equivalent to a modular transformation γ' which maps $\psi(x)$ to $(c'\tau + d')^{-k} \rho_{\mathbf{r}}(\gamma') \psi(x)$. Therefore, one obtains

$$\mathbf{X}_{\mathbf{r}} \rho_{\mathbf{r}}^*(\gamma) \mathbf{X}_{\mathbf{r}}^{-1} = \left(\frac{c'\tau + d'}{c\tau_{CP^{-1}}^* + d} \right)^{-k} \rho_{\mathbf{r}}(\gamma'). \quad (12)$$

Since $\mathbf{X}_{\mathbf{r}}$, $\rho_{\mathbf{r}}$ and $\rho_{\mathbf{r}'}$ are independent of τ , the overall coefficient on the right-hand side of Eq. (12) has to be a constant (complex) for non-zero weight k :

$$\frac{c'\tau + d'}{c\tau_{CP^{-1}}^* + d} = \frac{1}{\lambda^*}, \quad (13)$$

where $|\lambda| = 1$ due to the unitarity of $\rho_{\mathbf{r}}$ and $\rho_{\mathbf{r}'}$. The values of λ , c' and d' depend on γ .

Taking $\gamma = S$ ($c = 1, d = 0$), and denoting $c'(S) = C$, $d'(S) = D$ while keeping $\lambda(S) = \lambda$, we find $\tau = (\lambda\tau_{CP^{-1}}^* - D)/C$ from Eq. (13), and consequently,

$$\tau \xrightarrow{CP^{-1}} \tau_{CP^{-1}} = \lambda(C\tau^* + D), \quad \tau \xrightarrow{CP} \tau_{CP} = \frac{1}{C}(\lambda\tau^* - D). \quad (14)$$

Let us act with chain $CP \rightarrow T \rightarrow CP^{-1}$ on the modular τ itself:

$$\tau \xrightarrow{CP} \tau_{CP} = \frac{1}{C}(\lambda\tau^* - D) \xrightarrow{T} \frac{1}{C}(\lambda(\tau^* + 1) - D) \xrightarrow{CP^{-1}} \tau + \frac{\lambda}{C}. \quad (15)$$

The resulting transformation has to be a modular transformation, therefore λ/C is an integer. Since $|\lambda| = 1$, we find $|C| = 1$ and $\lambda = \pm 1$. After choosing the sign of C as $C = \mp 1$ so that $\text{Im}[\tau_{CP}] > 0$, the CP transformation of Eq. (14) turns to

$$\tau \xrightarrow{CP} n - \tau^*, \quad (16)$$

where n is an integer. The chain $CP \rightarrow S \rightarrow CP^{-1} = \gamma'(S)$ imposes no further restrictions on τ_{CP} . It is always possible to redefine the CP transformation in such a way that $n = 0$ by using the freedom of T transformation. Therefore, we can define the CP transformation of the modulus τ as

$$\tau \xrightarrow{CP} -\tau^*. \quad (17)$$

2.4 CP transformation of modular multiplets

Chiral superfields and modular forms transform in Eqs. (8) and (9), respectively, under a modular transformation. Chiral superfields also transform in Eq. (1) under the CP transformation. The CP transformation of modular forms was given in Ref. [113] as follows. Define a modular multiplet of the irreducible representation \mathbf{r} of Γ_N with weight k as $\mathbf{Y}_{\mathbf{r}}^{(k)}(\tau)$, which is transformed as:

$$\mathbf{Y}_{\mathbf{r}}^{(k)}(\tau) \xrightarrow{CP} \mathbf{Y}_{\mathbf{r}}^{(k)}(-\tau^*), \quad (18)$$

under the CP transformation. The complex conjugated CP transformed modular forms $\mathbf{Y}_{\mathbf{r}}^{(k)*}(-\tau^*)$ transform almost like the original multiplets $\mathbf{Y}_{\mathbf{r}}^{(k)}(\tau)$ under a modular transformation, namely:

$$\mathbf{Y}_{\mathbf{r}}^{(k)*}(-\tau^*) \xrightarrow{\gamma} \mathbf{Y}_{\mathbf{r}}^{(k)*}(-(\gamma\tau)^*) = (c\tau + d)^k \rho_{\mathbf{r}}^*(u(\gamma)) \mathbf{Y}_{\mathbf{r}}^{(k)*}(-\tau^*), \quad (19)$$

where $u(\gamma) \equiv CP\gamma CP^{-1}$. Using the consistency condition of Eq. (3), we obtain

$$\mathbf{X}_{\mathbf{r}}^T \mathbf{Y}_{\mathbf{r}}^{(k)*}(-\tau^*) \xrightarrow{\gamma} (c\tau + d)^k \rho_{\mathbf{r}}(\gamma) \mathbf{X}_{\mathbf{r}}^T \mathbf{Y}_{\mathbf{r}}^{(k)*}(-\tau^*). \quad (20)$$

Therefore, if there exist a unique modular multiplet at a level N , weight k and representation \mathbf{r} , which is satisfied for $N = 2-5$ with weight 2, we can express the modular form $\mathbf{Y}_{\mathbf{r}}^{(k)}(\tau)$ as:

$$\mathbf{Y}_{\mathbf{r}}^{(k)}(\tau) = \kappa \mathbf{X}_{\mathbf{r}}^T \mathbf{Y}_{\mathbf{r}}^{(k)*}(-\tau^*), \quad (21)$$

where κ is a proportional coefficient. Since $\mathbf{Y}_{\mathbf{r}}^{(k)}(-(-\tau^*)^*) = \mathbf{Y}_{\mathbf{r}}^{(k)}(\tau)$, Eq. (21) gives $\mathbf{X}_{\mathbf{r}}^* \mathbf{X}_{\mathbf{r}} = |\kappa|^2 \mathbf{1}_{\mathbf{r}}$. Therefore, the matrix $\mathbf{X}_{\mathbf{r}}$ is a symmetric one, and $\kappa = e^{i\phi}$ is a phase, which can be absorbed in the normalization of modular forms. In conclusion, the CP transformation of modular forms is given as:

$$\mathbf{Y}_{\mathbf{r}}^{(k)}(\tau) \xrightarrow{CP} \mathbf{Y}_{\mathbf{r}}^{(k)}(-\tau^*) = \mathbf{X}_{\mathbf{r}} \mathbf{Y}_{\mathbf{r}}^{(k)*}(\tau). \quad (22)$$

It is also emphasized that $\mathbf{X}_{\mathbf{r}} = \mathbf{1}_{\mathbf{r}}$ satisfies the consistency condition Eq. (3) in a basis that generators of S and T of Γ_N are represented by symmetric matrices because of $\rho_{\mathbf{r}}^*(S) = \rho_{\mathbf{r}}^\dagger(S) = \rho_{\mathbf{r}}(S^{-1}) = \rho_{\mathbf{r}}(S)$ and $\rho_{\mathbf{r}}^*(T) = \rho_{\mathbf{r}}^\dagger(T) = \rho_{\mathbf{r}}(T^{-1})$.

The CP transformations of chiral superfields and modular multiplets are summarized as follows:

$$\tau \xrightarrow{CP} -\tau^*, \quad \psi(x) \xrightarrow{CP} X_r \bar{\psi}(x_P), \quad \mathbf{Y}_{\mathbf{r}}^{(k)}(\tau) \xrightarrow{CP} \mathbf{Y}_{\mathbf{r}}^{(k)}(-\tau^*) = \mathbf{X}_{\mathbf{r}} \mathbf{Y}_{\mathbf{r}}^{(k)*}(\tau), \quad (23)$$

where $\mathbf{X}_{\mathbf{r}} = \mathbf{1}_{\mathbf{r}}$ can be taken in the basis of symmetric generators of S and T . We use this CP transformation of modular forms to construct the CP invariant mass matrices in the next section.

3 CP invariant lepton mass matrix in A_4 modular symmetry

In this section, we propose the CP invariant lepton mass matrix for introducing the A_4 modular symmetry. The three generations of the left-handed lepton doublets are assigned to be an A_4 triplet L , and the right-handed charged leptons e^c , μ^c , and τ^c are A_4 singlets $\mathbf{1}$, $\mathbf{1}''$, and $\mathbf{1}'$, respectively. The three generations of the right-handed neutrinos are also assigned to be an A_4 triplet N^c . The weight of the superfields of left-handed leptons is fixed to be -1 as a standard. The weight of right-handed neutrinos is also taken to be -1 in order to give a Dirac neutrino mass matrix in terms of modular forms of weight 2. On the other hand, weights of the right-handed charged leptons e^c , μ^c , and τ^c are put (k_e, k_μ, k_τ) in general. Weights of Higgs fields H_u, H_d are fixed to be 0. The representations and weights for MSSM fields and modular forms of weight k are summarized in Table 1.

	L	(e^c, μ^c, τ^c)	N^c	H_u	H_d	$Y_{\mathbf{3}}^{(k)}$
$SU(2)$	$\mathbf{2}$	$\mathbf{1}$	$\mathbf{1}$	$\mathbf{2}$	$\mathbf{2}$	$\mathbf{1}$
A_4	$\mathbf{3}$	$(\mathbf{1}, \mathbf{1}'', \mathbf{1}')$	$\mathbf{3}$	$\mathbf{1}$	$\mathbf{1}$	$\mathbf{3}$
weight	-1	(k_e, k_μ, k_τ)	-1	0	0	k

Table 1: Representations and weights for MSSM fields and relevant modular forms of weight k .

Since we construct the CP invariant lepton mass matrices with minimum number of parameters, we fix weights $k_e = -1$, $k_\mu = -3$, $k_\tau = -5$ for right-handed charged leptons. Then, we need modular forms of weight 2, 4 and 6, $Y_{\mathbf{3}}^{(2)}$, $Y_{\mathbf{3}}^{(4)}$ and $Y_{\mathbf{3}}^{(6)}$. For weight 4, there are five modular forms two singlets and one triplet of A_4 . Those are given in terms of weight 2 modular forms $Y_1(\tau)$, $Y_2(\tau)$ and $Y_3(\tau)$ as:

$$\begin{aligned}
 Y_{\mathbf{1}}^{(4)}(\tau) &= Y_1(\tau)^2 + 2Y_2(\tau)Y_3(\tau), & Y_{\mathbf{1}'}^{(4)}(\tau) &= Y_3(\tau)^2 + 2Y_1(\tau)Y_2(\tau), \\
 Y_{\mathbf{1}''}^{(4)}(\tau) &= Y_2(\tau)^2 + 2Y_1(\tau)Y_3(\tau) = 0, & Y_{\mathbf{3}}^{(4)}(\tau) &= \begin{pmatrix} Y_1^{(4)}(\tau) \\ Y_2^{(4)}(\tau) \\ Y_3^{(4)}(\tau) \end{pmatrix} = \begin{pmatrix} Y_1(\tau)^2 - Y_2(\tau)Y_3(\tau) \\ Y_3(\tau)^2 - Y_1(\tau)Y_2(\tau) \\ Y_2(\tau)^2 - Y_1(\tau)Y_3(\tau) \end{pmatrix}. \quad (24)
 \end{aligned}$$

For the weight 6, we have seven modular forms, one singlet and two triplets of A_4 as:

$$\begin{aligned}
 Y_{\mathbf{1}}^{(6)} &= Y_1^3 + Y_2^3 + Y_3^3 - 3Y_1Y_2Y_3, \\
 Y_{\mathbf{3}}^{(6)} &\equiv \begin{pmatrix} Y_1^{(6)} \\ Y_2^{(6)} \\ Y_3^{(6)} \end{pmatrix} = (Y_1^2 + 2Y_2Y_3) \begin{pmatrix} Y_1 \\ Y_2 \\ Y_3 \end{pmatrix}, & Y_{\mathbf{3}'}^{(6)} &\equiv \begin{pmatrix} Y_1'^{(6)} \\ Y_2'^{(6)} \\ Y_3'^{(6)} \end{pmatrix} = (Y_3^2 + 2Y_1Y_2) \begin{pmatrix} Y_3 \\ Y_1 \\ Y_2 \end{pmatrix}. \quad (25)
 \end{aligned}$$

Then, the A_4 invariant superpotential of the charged leptons, w_E , by taking into account the modular weights is obtained as

$$w_E = \alpha_e e^c H_d Y_{\mathbf{3}}^{(2)} L + \beta_e \mu^c H_d Y_{\mathbf{3}}^{(4)} L + \gamma_e \tau^c H_d Y_{\mathbf{3}}^{(6)} L + \gamma_e' \tau^c H_d Y_{\mathbf{3}'}^{(6)} L, \quad (26)$$

where $\alpha_e, \beta_e, \gamma_e$, and γ_e' are constant parameters. Under CP, the superfields transform as:

$$e^c \xrightarrow{CP} X_{\mathbf{1}}^* \bar{e}^c, \quad \mu^c \xrightarrow{CP} X_{\mathbf{1}''}^* \bar{\mu}^c, \quad \tau^c \xrightarrow{CP} X_{\mathbf{1}'}^* \bar{\tau}^c, \quad L \xrightarrow{CP} X_{\mathbf{3}} \bar{L}, \quad H_d \xrightarrow{CP} \eta_d \bar{H}_d, \quad (27)$$

and we can take $\eta_d = 1$ without loss of generality. Since the representations of S and T are symmetric (see Appendic A), we can choose $X_{\mathbf{3}} = \mathbf{1}$ and $X_{\mathbf{1}} = X_{\mathbf{1}'} = X_{\mathbf{1}''} = \mathbf{1}$ as discussed in Eq. (23).

Taking (e_L, μ_L, τ_L) in the flavor base, the charged lepton mass matrix M_E is simply written as:

$$M_E(\tau) = v_d \begin{pmatrix} \alpha_e & 0 & 0 \\ 0 & \beta_e & 0 \\ 0 & 0 & \gamma_e \end{pmatrix} \begin{pmatrix} Y_1(\tau) & Y_3(\tau) & Y_2(\tau) \\ Y_2^{(4)}(\tau) & Y_1^{(4)}(\tau) & Y_3^{(4)}(\tau) \\ Y_3^{(6)}(\tau) + g_e Y_3'^{(6)}(\tau) & Y_2^{(6)}(\tau) + g_e Y_2'^{(6)}(\tau) & Y_1^{(6)}(\tau) + g_e Y_1'^{(6)}(\tau) \end{pmatrix}_{RL}, \quad (28)$$

where $g_e = \gamma_e'/\gamma_e$, and v_d is VEV of the neutral component of H_d . The coefficients α_e, β_e and γ_e are taken to be real without loss of generality. Under CP transformation, the mass matrix M_E is transformed following from Eq. (28) as:

$$M_E(\tau) \xrightarrow{CP} M_E(-\tau^*) = M_E^*(\tau) = v_d \begin{pmatrix} \alpha_e & 0 & 0 \\ 0 & \beta_e & 0 \\ 0 & 0 & \gamma_e \end{pmatrix} \begin{pmatrix} Y_1(\tau)^* & Y_3(\tau)^* & Y_2(\tau)^* \\ Y_2^{(4)}(\tau)^* & Y_1^{(4)}(\tau)^* & Y_3^{(4)}(\tau)^* \\ Y_3^{(6)}(\tau)^* + g_e^* Y_3'^{(6)}(\tau)^* & Y_2^{(6)}(\tau)^* + g_e^* Y_2'^{(6)}(\tau)^* & Y_1^{(6)}(\tau)^* + g_e^* Y_1'^{(6)}(\tau)^* \end{pmatrix}_{RL}. \quad (29)$$

Let us discuss the neutrino sector. In Table 1, the A_4 invariant superpotential for the neutrino sector, w_ν , is given as:

$$\begin{aligned} w_\nu &= w_D + w_N, \\ w_D &= \gamma_\nu N^c H_u Y_{\mathbf{3}}^{(2)} L + \gamma_\nu' N^c H_u Y_{\mathbf{3}}'^{(2)} L, \\ w_N &= \Lambda N^c N^c Y_{\mathbf{3}}^{(2)}. \end{aligned} \quad (30)$$

where γ_ν and γ_ν' are Yukawa couplings, and Λ denotes a right-handed Majorana neutrino mass scale. By putting v_u for VEV of the neutral component of H_u and taking $(\nu_e, \nu_\mu, \nu_\tau)$ for neutrinos, the Dirac neutrino mass matrix, M_D , is obtained as

$$M_D = \gamma_\nu v_u \begin{pmatrix} 2Y_1 & (-1 + g_D)Y_3 & (-1 - g_D)Y_2 \\ (-1 - g_D)Y_3 & 2Y_2 & (-1 + g_D)Y_1 \\ (-1 + g_D)Y_2 & (-1 - g_D)Y_1 & 2Y_3 \end{pmatrix}_{RL}, \quad (31)$$

where $g_D = \gamma_\nu'/\gamma_\nu$. On the other hand the right-handed Majorana neutrino mass matrix, M_N is written as follows:

$$M_N = \Lambda \begin{pmatrix} 2Y_1 & -Y_3 & -Y_2 \\ -Y_3 & 2Y_2 & -Y_1 \\ -Y_2 & -Y_1 & 2Y_3 \end{pmatrix}_{RR}. \quad (32)$$

By using the type-I seesaw mechanism, the effective neutrino mass matrix, M_ν is obtained as

$$M_\nu = M_D^T M_N^{-1} M_D. \quad (33)$$

In a CP conserving modular invariant theory, both CP and modular symmetries are broken spontaneously by VEV of the modulus τ . However, there exist certain values of τ which conserve CP while breaking the modular symmetry. Obviously, this is the case if τ is left invariant by CP, i.e.

$$\tau \xrightarrow{CP} -\tau^* = \tau, \quad (34)$$

which indicates τ lies on the imaginary axis, $\text{Re}[\tau] = 0$. In addition to $\text{Re}[\tau] = 0$, CP is conserved at the boundary of the fundamental domain.

Due to Eq. (23), one then has

$$M_E(\tau) = M_E^*(\tau), \quad M_\nu(\tau) = M_\nu^*(\tau), \quad (35)$$

if g_e and g_D are taken to be real. Therefore, the source of the CP violation is only non-trivial $\text{Re}[\tau]$ after breaking the modular symmetry. In the next section, we present a numerical analysis of the CP violation by fixing the modulus τ with real g_e and g_D .

4 Numerical results of leptonic CP violation

We have presented the CP invariant lepton mass matrices in the A_4 modular symmetry. The tiny neutrino masses are given via type-I seesaw. The CP symmetry is broken spontaneously by VEV of the modulus τ . Thus, VEV of τ breaks the CP invariance as well as the modular invariance. The source of the CP violation is the real part of τ . Indeed, the spontaneous CP violation is realized by fixing τ . Then, the Dirac CP phase and Majorana phases are predicted clearly with reproducing observed lepton mixing angles and two neutrino mass squared differences. The predictive CP phases are possibly linked to the phase of the leptogenesis [116].

Our parameters are real ones $\alpha_e, \beta_e, \gamma_e, \gamma'_e, \gamma_\nu, \gamma'_\nu$ and Λ in addition to the complex τ . Observed input data are three charged lepton masses, three flavor mixing angles and two neutrino mass squared differences. Since γ_ν and Λ appear only with the combination γ_ν^2/Λ in the neutrino mass matrix, the input data determine completely our parameters apart from error-bars of the experimental data. Therefore, the lepton mixing angles, the Dirac phase and Majorana phases are predicted in the restricted ranges.

As the input charged lepton masses, we take Yukawa couplings of charged leptons at the GUT scale 2×10^{16} GeV, where $\tan \beta = 5$ is taken as a bench mark [131, 132]:

$$y_e = (1.97 \pm 0.024) \times 10^{-6}, \quad y_\mu = (4.16 \pm 0.050) \times 10^{-4}, \quad y_\tau = (7.07 \pm 0.073) \times 10^{-3}, \quad (36)$$

where lepton masses are given by $m_\ell = y_\ell v_H$ with $v_H = 174$ GeV.

observable	best fit $\pm 1 \sigma$ for NH	best fit $\pm 1 \sigma$ for IH
$\sin^2 \theta_{12}$	$0.304^{+0.012}_{-0.012}$	$0.304^{+0.013}_{-0.012}$
$\sin^2 \theta_{23}$	$0.573^{+0.016}_{-0.020}$	$0.575^{+0.016}_{-0.019}$
$\sin^2 \theta_{13}$	$0.02219^{+0.00062}_{-0.00063}$	$0.02238^{+0.00063}_{-0.00062}$
Δm_{sol}^2	$7.42^{+0.21}_{-0.20} \times 10^{-5} \text{eV}^2$	$7.42^{+0.21}_{-0.20} \times 10^{-5} \text{eV}^2$
Δm_{atm}^2	$2.517^{+0.026}_{-0.028} \times 10^{-3} \text{eV}^2$	$-2.498^{+0.028}_{-0.028} \times 10^{-3} \text{eV}^2$

Table 2: The best fit $\pm 1 \sigma$ of neutrino parameters from NuFIT 5.0 for NH and IH [133].

We also input the lepton mixing angles and neutrino mass parameters which are given by NuFit 5.0 in Table 2 [133]. In our analysis, the Dirac CP phase δ_{CP} (see Appendix C) is output because its observed range is too wide at 3σ confidence level. We investigate two possible cases of neutrino

masses m_i , which are the normal hierarchy (NH), $m_3 > m_2 > m_1$, and the inverted hierarchy (IH), $m_2 > m_1 > m_3$. Neutrino masses and the PMNS matrix U_{PMNS} [118, 119] are obtained by diagonalizing $M_E^\dagger M_E$ and $M_\nu^\dagger M_\nu$. We also investigate the effective mass for the $0\nu\beta\beta$ decay, $\langle m_{ee} \rangle$ (see Appendix C) and the sum of three neutrino masses $\sum m_i$ since it is constrained by the recent cosmological data, which is the upper-bound $\sum m_i \leq 120$ meV obtained at the 95% confidence level [115, 134].

Let us discuss numerical results for NH of neutrino masses. We scan τ in the fundamental domain of $SL(2, Z)$. The real parameters g_e and g_D are scanned in $[-10, 10]$. As a measure of good-fit, we adopt the sum of one-dimensional χ^2 functions for five accurately known observables Δm_{atm}^2 , Δm_{sol}^2 , $\sin^2 \theta_{12}$, $\sin^2 \theta_{23}$ and $\sin^2 \theta_{13}$ in NuFit 5.0 [133]. In addition, we employ Gaussian approximations for fitting m_e , m_μ and m_τ .

In Fig. 1, we show the allowed region on the $\text{Re}[\tau] - \text{Im}[\tau]$ plane, where three mixing angles, Δm_{atm}^2 , Δm_{sol}^2 and charged lepton masses are consistent with observed ones. The green and magenta regions correspond to $\sqrt{\chi^2} \leq 2$ and 3, respectively. The predicted range of τ is in $\text{Re}[\tau] = \pm[0.1, 0.5]$ and $\text{Im}[\tau] = [0.96, 1.30]$ at $\sqrt{\chi^2} \leq 3$ (magenta).

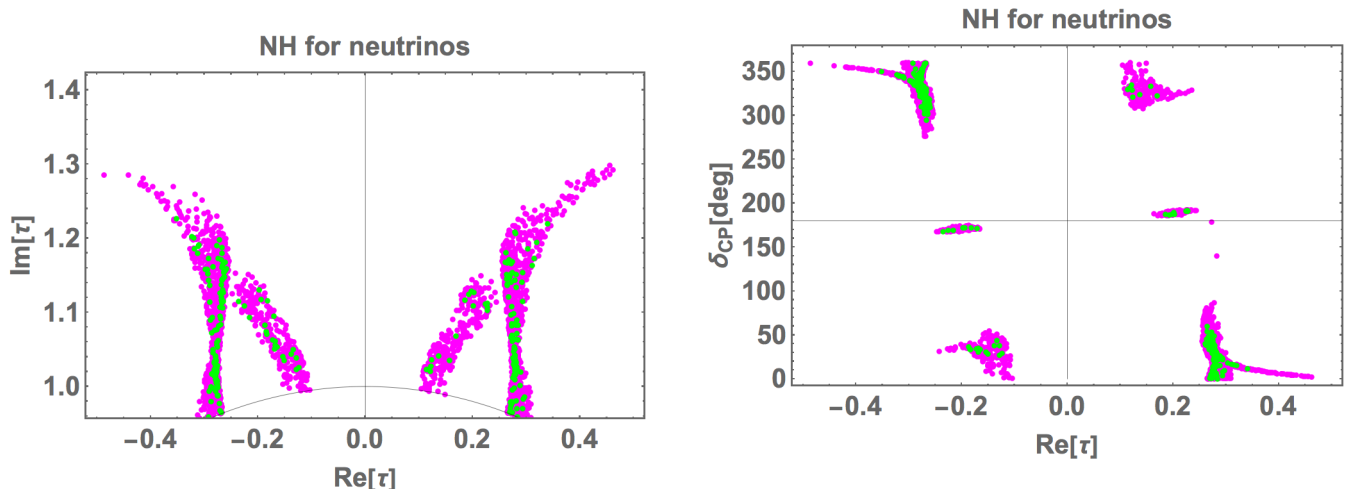


Figure 1: Allowed regions of τ for NH, where green and magenta points correspond to $\sqrt{\chi^2} \leq 2$ and 3, respectively. The solid curve is the boundary of the fundamental domain, $|\tau| = 1$.

Figure 2: Prediction of Dirac phase δ_{CP} versus $\text{Re}[\tau]$ for NH. There are six regions, which are almost symmetric with respect to the point $(\text{Re}[\tau] = 0, \delta_{CP} = 180^\circ)$. Colors denote same ones in Fig. 1.

Due to the rather broad range of $\text{Re}[\tau]$, the predictive Dirac CP phase δ_{CP} , which is defined in Appendix C, is not so restricted. In Fig. 2, we show a prediction of δ_{CP} versus $\text{Re}[\tau]$. It is remarked that δ_{CP} is predicted in six regions depending on the sign of $\text{Re}[\tau]$. Those are $[0^\circ, 50^\circ]$, $[170^\circ, 175^\circ]$, $[280^\circ, 360^\circ]$ for $\text{Re}[\tau] < 0$, and $[0^\circ, 80^\circ]$, $[185^\circ, 190^\circ]$, $[310^\circ, 360^\circ]$ for $\text{Re}[\tau] > 0$ at $\sqrt{\chi^2} \leq 3$ (magenta). These are almost symmetric with respect to the point $(\text{Re}[\tau] = 0, \delta_{CP} = 180^\circ)$. This prediction is consistent with the result of global fit of NuFit 5.0 [133]:

$$\delta_{CP} = 197^\circ_{-24^\circ}^{+27^\circ}. \quad (37)$$

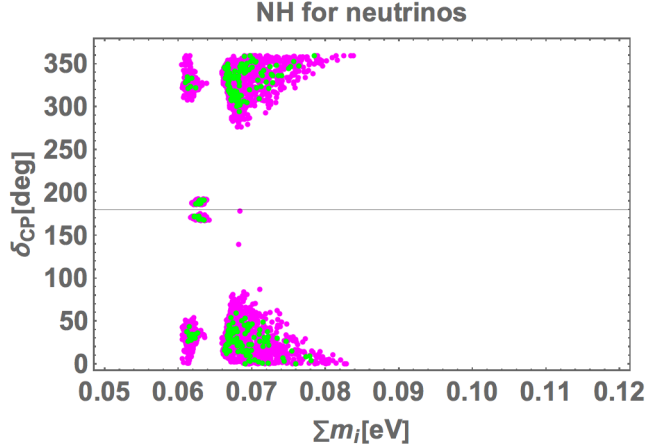


Figure 3: Predicted six regions of Dirac phase δ_{CP} versus the sum of neutrino masses $\sum m_i$ for NH. Colors denote same ones in Fig. 1.

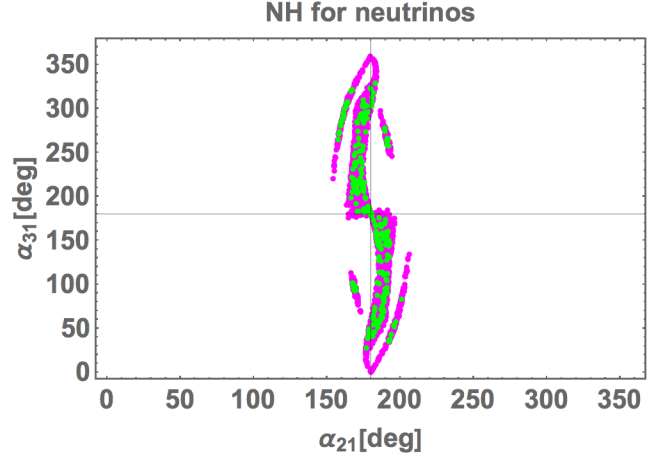


Figure 4: Predicted Majorana phases α_{21} and α_{31} for NH. Colors denote same ones in Fig. 1.

In Fig. 3, we show a prediction of δ_{CP} versus $\sum m_i$. It is also found different six predicted regions. The sum of neutrino masses $\sum m_i$ is restricted in the narrow range $[60, 84]$ meV at $\sqrt{\chi^2} \leq 3$ (magenta). It is consistent with the cosmological bound 120 meV in the minimal cosmological model, $\Lambda\text{CDM} + \sum m_i$. [115, 134].

In Fig. 4, we show the prediction of Majorana phases α_{21} and α_{31} , which are defined by Appendix C. The predicted α_{21} is around 180° , but α_{31} is distributed in the full range of $[0^\circ, 360^\circ]$ at $\sqrt{\chi^2} \leq 3$ (magenta).

We can calculate the effective mass $\langle m_{ee} \rangle$ for the $0\nu\beta\beta$ decay by using the Dirac CP phase and Majorana phases as seen in Appendix C. The predicted $\langle m_{ee} \rangle$ is

$$\langle m_{ee} \rangle = [0.003, 3] \text{ meV}, \quad (38)$$

at $\sqrt{\chi^2} \leq 3$. It is difficult to reach this value in the future experiments of the neutrinoless double beta decay.

We have checked the correlation between three mixing angles and δ_{CP} plane. The predicted δ_{CP} is correlated weakly with $\sin^2 \theta_{23}$ in our model. It has the broadest ranges of $[0^\circ, 80^\circ]$ and $[280^\circ, 360^\circ]$ at the best fit value of $\sin^2 \theta_{23} = 0.573$, but ranges of $[0^\circ, 30^\circ]$ and $[330^\circ, 360^\circ]$ are excluded near the observed upper bound of $\sin^2 \theta_{23}$. On the other hand, there are no correlations among $\sin^2 \theta_{12}$, $\sin^2 \theta_{13}$ and δ_{CP} .

We show the best fit sample for NH in Table 3, where numerical values of parameters and output are listed. As a measure of goodness of fit, we show square root of the sum of one-dimensional χ^2 functions.

We have also scanned the parameter space for the case of IH of neutrino masses. We have found parameter sets which reproduce the observed masses and three mixing angles $\sin^2 \theta_{23}$, $\sin^2 \theta_{12}$, and $\sin^2 \theta_{13}$ at $\sqrt{\chi^2} \leq 5$. However, there is no parameter sets below $\sqrt{\chi^2} = 4$.

The allowed region of τ is restricted in the narrow regions. As shown in Fig. 5, the predicted range of $\text{Im}[\tau]$ is $[1.15, 1.16]$ at $\sqrt{\chi^2} = 4-5$ and $\text{Re}[\tau]$ is close to ± 0.5 .

	NH	IH
τ	$-0.2637 + 1.1549 i$	$0.4984 + 1.1553 i$
g_D	-1.29	1.74
g_e	-1.01	1.68×10^{-7}
β_e/α_e	4.66×10^{-2}	3.64×10^{-2}
γ_e/α_e	11.9	7.35×10^{-4}
$\sin^2 \theta_{12}$	0.305	0.309
$\sin^2 \theta_{23}$	0.571	0.494
$\sin^2 \theta_{13}$	0.0220	0.0222
δ_{CP}	317°	300°
$[\alpha_{21}, \alpha_{31}]$	$[189^\circ, 64^\circ]$	$[116^\circ, 270^\circ]$
$\sum m_i$	67.3 meV	145 meV
$\langle m_{ee} \rangle$	0.18 meV	35.5 meV
$\sqrt{\chi^2}$	1.39	4.27

Table 3: Numerical values of parameters and observables at the best fit points of NH and IH.

In Fig. 6, we show the allowed region on the $\text{Re}[\tau] - \delta_{CP}$ plane. The predicted δ_{CP} is severely restricted as in $[50^\circ, 70^\circ]$ and $[290^\circ, 310^\circ]$. This prediction is consistent with the result of global fit of IH in NuFit 5.0, $\delta_{CP} = 282^\circ_{-30^\circ}^{+26^\circ}$. In addition, $\sin^2 \theta_{23}$ is restricted in $[0.505, 0.515]$ [133].

On the other hand, the sum of neutrino masses $\sum m_i$ is restricted in the narrow range $[143, 147]$ meV at $\sqrt{\chi^2} = 4-5$. Therefore, the case of IH will be excluded by the improved cosmological bound in the near future. The predicted $\langle m_{ee} \rangle$ is given as $\langle m_{ee} \rangle = [35, 36]$ meV.

We also present the best fit set of IH in Table 3, where values of relevant parameters are listed compared with the values of the NH case.

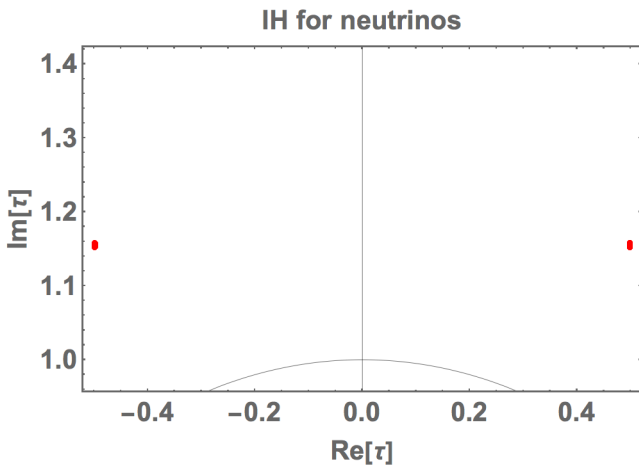


Figure 5: Allowed regions of τ for IH at $\sqrt{\chi^2} = 4-5$.

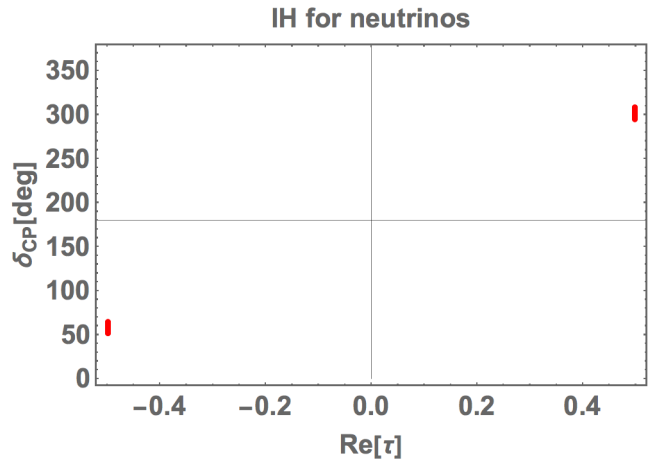


Figure 6: Prediction of Dirac phase δ_{CP} versus $\text{Re}[\tau]$ for IH at $\sqrt{\chi^2} = 4-5$

In our numerical calculations, we have not included the RGE effects in the lepton mixing angles. We suppose that those corrections are very small between the electroweak and GUT scales. This assumption is justified well in the case of $\tan \beta \leq 10$ unless neutrino masses are almost degenerate [27].

We have presented CP invariant lepton mass matrices with minimum number of parameters by fixing weights ($k_e = -1$, $k_\mu = -3$, $k_\tau = -5$) for right-handed charged leptons. Therefore, the charged lepton mass matrix is given by modular forms of weight 2, 4 and 6, $Y_{\mathbf{3}}^{(2)}$, $Y_{\mathbf{3}}^{(4)}$ and $Y_{\mathbf{3}}^{(6)}$. However, this choice for weights is not a unique one even if we consider the seesaw model with minimum number of parameters. We have examined alternative three choices: ($k_e = -1$, $k_\mu = -1$, $k_\tau = -5$), ($k_e = -1$, $k_\mu = -1$, $k_\tau = -7$) and ($k_e = -1$, $k_\mu = -3$, $k_\tau = -7$). The corresponding charged lepton mass matrices are presented in Appendix D. In those three models, we have also obtained successful numerical results, which are not so different from above ones. We present samples of parameter sets for each model in Appendix D for NH of neutrino masses. The cases of IH are omitted since their $\sqrt{\chi^2}$ are larger than 4. Our study of the leptogenesis is focused on the case of weights ($k_e = -1$, $k_\mu = -3$, $k_\tau = -5$) in the next section.

5 Leptogenesis

The BAU at the present universe is measured very precisely by the cosmic microwave background radiation as [115]:

$$Y_B = \frac{n_B}{s} = (0.852 - 0.888) \times 10^{-10}, \quad (39)$$

at 3σ confidence level, where Y_B is defined by the ratio between the number density of baryon asymmetry n_B and the entropy density s . One of the most attractive scenarios for baryogenesis is the canonical leptogenesis scenario [116] in which the decays of right-handed neutrinos can generate the lepton asymmetry that is partially converted into the baryon asymmetry via the sphaleron process [117]. The sign and magnitude of the BAU are predicted by the masses and Yukawa coupling constants of right-handed neutrinos. If their masses are hierarchical, the lightest one must be $\mathcal{O}(10^9)$ GeV [135] to explain the BAU. The sign of the BAU depends on the CP phase structure in the lepton mass matrices. In general, the sign of the BAU cannot be predicted uniquely even if the Dirac and Majorana CP phases are determined. This is because there exist generally one or more additional phases associated with right-handed neutrinos which decouple from the low energy phenomena even if right-handed neutrinos are sufficiently heavy. However, our predictive Dirac and Majorana CP phases are linked to the BAU because the CP violation is originated from only τ in our model with A_4 modular symmetry.

Let us discuss the leptogenesis by decays of right-handed neutrinos in our model. Since the mass ratios of right-handed neutrinos are not so large, and then we have to include the effects of all three right-handed neutrinos to the leptogenesis. For simplicity, we assume that the reheating temperature of inflation is sufficiently higher than the mass of the heaviest right-handed neutrino and that the initial abundances of all right-handed neutrinos are zero. On the other hand, the mass degeneracy of the right-handed neutrinos is not so large, and so the resonant enhancement of the leptogenesis [136, 137] does not occur. Thus, we shall use the formalism based on the Boltzmann equations to estimate the asymmetries. Moreover, as we show below, the required masses of right-handed neutrinos are $\mathcal{O}(10^{13})$ GeV, and so we can apply the simple one-flavor approximation of the leptogenesis. Therefore, we neglect the so-called flavor effect [138–145]. Furthermore, to achieve successful leptogenesis via the decay of such heavy right-handed neutrinos, the reheating temperature must be higher than

$\mathcal{O}(10^{13})$ GeV. In the framework of supersymmetry (SUSY), such high reheating temperature can cause the overproduction of gravitinos, which is called the gravitino problem [146, 147]. However, in our scenario, we assume that SUSY is broken at close to the Planck scale. In this situation, SUSY particles, including the gravitino, have masses around the Planck scale. Therefore, gravitino cannot be thermally produced after inflation. So the constraint on the reheating temperature due to the gravitino problem can be eliminated.

The flavor structure of our model appears in the CP asymmetry parameter ε_I , which is:

$$\varepsilon_I = \frac{\Gamma(N_I \rightarrow L + \overline{H}_u) - \Gamma(N_I \rightarrow \overline{L} + H_u)}{\Gamma(N_I \rightarrow L + \overline{H}_u) + \Gamma(N_I \rightarrow \overline{L} + H_u)}. \quad (40)$$

It is proportional to the imaginary part of Yukawa couplings as:

$$\varepsilon_I \propto \sum_{J \neq I} \text{Im}\{(y_\nu y_\nu^\dagger)_{IJ}\}^2. \quad (41)$$

Here, $y_\nu y_\nu^\dagger$ is given by the Dirac neutrino mass matrix M_D in the real diagonal base of the right-handed Majorana neutrino mass matrix M_N as follows:

$$y_\nu y_\nu^\dagger = \frac{1}{v_u^2} V_R^\dagger (M_D M_D^\dagger) V_R, \quad \text{with} \quad V_R^\dagger (M_N M_N^\dagger) V_R = \text{diag}(M_1^2, M_2^2, M_3^2), \quad (42)$$

where M_D and M_N are given in Eqs. (31) and (32), respectively, and M_1, M_2 and M_3 are real.

The Boltzmann equations are then solved numerically and the total lepton asymmetry Y_L from the decays of right-handed neutrinos is estimated. The present baryon asymmetry can be estimated as $Y_B = -8/23 Y_L$ for the two Higgs doublets (see Appendix E).

In our model, the phases in the PMNS matrix and the high energy phases associated with right-handed neutrinos are originated in the modulus τ . In this situation, there may exist the correlations between the phases in the PMNS matrix and the yield of the BAU.

Since the best-fit point of the modulus τ is rather close to the fixed point $\tau = i$ for NH as seen in Table 3, we can calculate approximately the asymmetry parameter ε_I of Eq.(41) in terms of a small complex parameter ϵ , which is defined as $\tau = i + \epsilon$ in perturbation. This analytic calculation is possible due to the simple Dirac neutrino mass matrix at $\tau = i$. It is found that the leading term of $\text{Im}\{(y_\nu y_\nu^\dagger)_{IJ}\}^2$ is given by $\text{Im}[\epsilon^2]$. On the other hand, it is almost impossible to give an approximate form of the CP phase δ_{CP} or the CP violating measure J_{CP} at low energy. Since the right-handed Majorana neutrino mass matrix M_N gives one massless and two degenerated masses at $\tau = i$ in our model, its inverse is a singular one at $\tau = i$. After seesaw, the left-handed Majorana mass matrix is unstable at nearby $\tau = i$ for perturbation. Indeed, we could not obtain a reliable analytic expression for J_{CP} . Therefore, we study the correlations between the CP phase δ_{CP} and the yield of the BAU in numerical calculations.

6 Baryon asymmetry

Let us then show the results of the BAU by right-handed neutrinos in our model by using parameter sets of section 4 at $\sqrt{\chi^2} \leq 3$ for NH of neutrino masses. At first, we discuss the sign of the BAU produced by right-handed neutrinos in the model. The sign of the BAU is determined by the τ and

the sign of the real parameter g_D as shown in Fig. 7. In order to obtain the observed positive Y_B (orange points), the region of $(\text{Re}[\tau] < 0, g_D < 0)$ or $(\text{Re}[\tau] > 0, g_D > 0)$ is required.

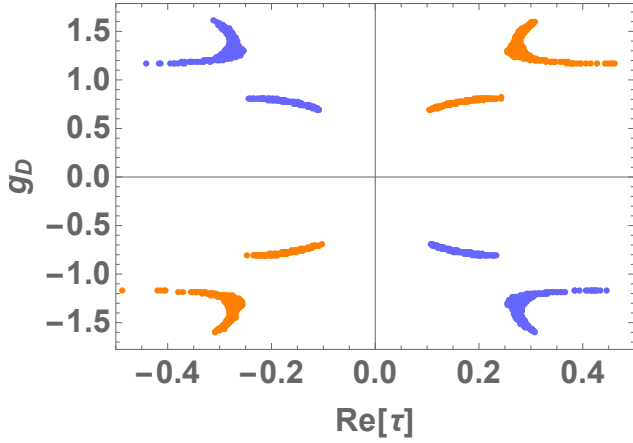


Figure 7: The sign of Y_B and regions of $\text{Re}[\tau]$ – g_D . Orange and blue points denote positive and negative Y_B , respectively. Points correspond to the output of section 4 at $\sqrt{\chi^2} \leq 3$

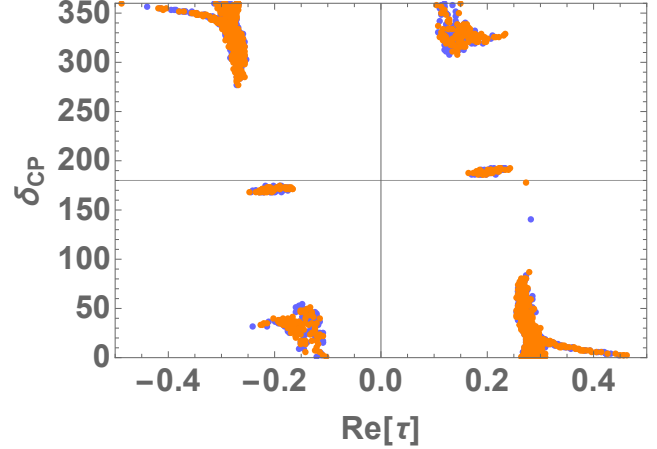


Figure 8: Predictive δ_{CP} versus $\text{Re}[\tau]$. Blue color points (negative Y_B) almost overlap with orange ones (positive Y_B). Points correspond to the output of section 4 at $\sqrt{\chi^2} \leq 3$

In order to see the link between the sign of Y_B and the predictive Dirac CP phase, we show the predictive δ_{CP} versus $\text{Re}[\tau]$ for the positive (orange) and negative (blue) Y_B in Fig. 8, which is essentially same one in Fig. 2 apart from the sign of Y_B . All six predicted regions of the $\text{Re}[\tau]$ – δ_{CP} plane can give both positive (orange) and negative (blue) Y_B by the choice of the relevant sign of g_D .

Indeed, we can see this situation in Fig. 9, where the positive (orange) and negative (blue) signs of Y_B are shown in the g_D – δ_{CP} plane. The positive and negative regions of Y_B are clearly separated.

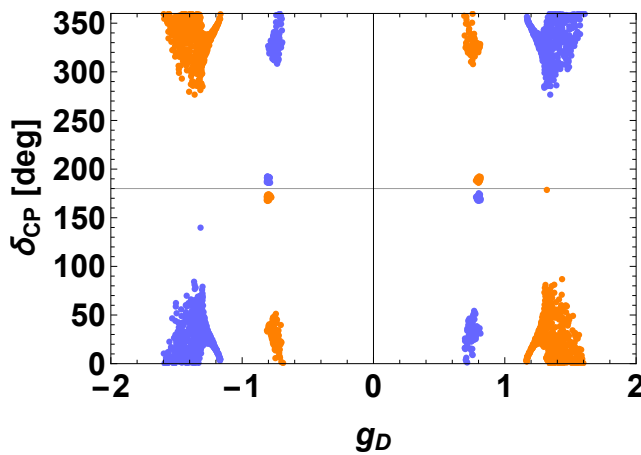


Figure 9: The sign of Y_B in the g_D – δ_{CP} plane. Orange and blue points denote positive Y_B and negative Y_B , respectively.

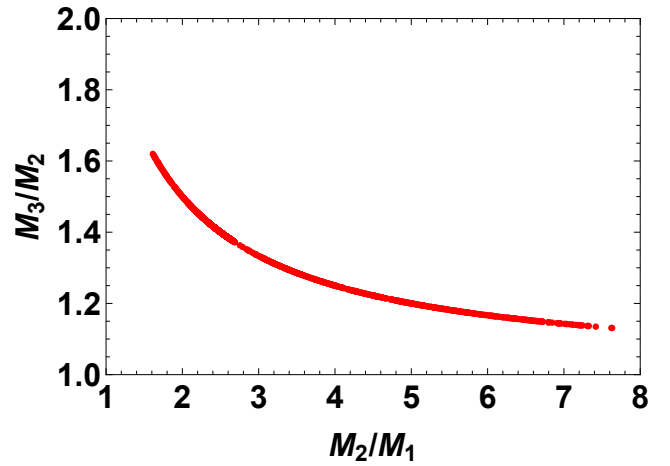


Figure 10: The allowed curve of ratios of right-handed Majorana masses in the M_2/M_1 – M_3/M_2 plane.

Next, we discuss the magnitude of the BAU yield. The yield of the BAU depends on the masses M_i and Yukawa coupling constants of right-handed neutrinos. These parameters are highly restricted due to the symmetry in our model. First, the allowed range of the mass ratios of right-handed neutrinos is shown in Fig. 10. It is found that M_3/M_2 decreases on the curve in the range of $[1.1, 1.6]$ depending on $M_2/M_1 = [1.6, 7.6]$. Those mass ratios suggest that all three right-handed neutrinos should be taken into account in the calculation of the leptogenesis.

We find that the yield can be at most the same order of the observed value of the BAU in Eq. (39). This is because the model predicts a relatively large value of the effective neutrino mass of the leptogenesis \tilde{m}_1 which is defined as $\tilde{m}_1 = (y_\nu y_\nu^\dagger)_{11} v_u^2 / M_1$. We show the predictive Y_B in the \tilde{m}_1 - M_1 plane in Fig. 11, where four predictive ranges of Y_B are discriminated by colors. We find numerically $\tilde{m}_1 \simeq 40$ meV or $\tilde{m}_1 \simeq 60$ meV, and then the strong wash-out effect is inevitable. In order to obtain the observed BAU, $\tilde{m}_1 = [60, 61]$ meV and $M_1 = [1.5, 6.5] \times 10^{13}$ GeV are required as seen in Fig. 11. It is an important consequence that the lightest right-handed neutrino mass should be in the restricted range. Thus, the absolute values of right-handed neutrino masses can be determined from the BAU.

We show predictive Y_B versus M_1 in Fig. 12, where M_1 is taken to be $\mathcal{O}(10^{13})$ GeV. The predictive Y_B is rather broad in this range of M_1 . Especially, it expands maximally at $M_1 = 3.36 \times 10^{13}$ GeV. That is because the larger M_1 is, the more the wash-out effect of the $\Delta L = 2$ processes is important. Thereby, the lightest right-handed neutrino mass is restricted to the specific range $M_1 = [1.5, 6.5] \times 10^{13}$ GeV.

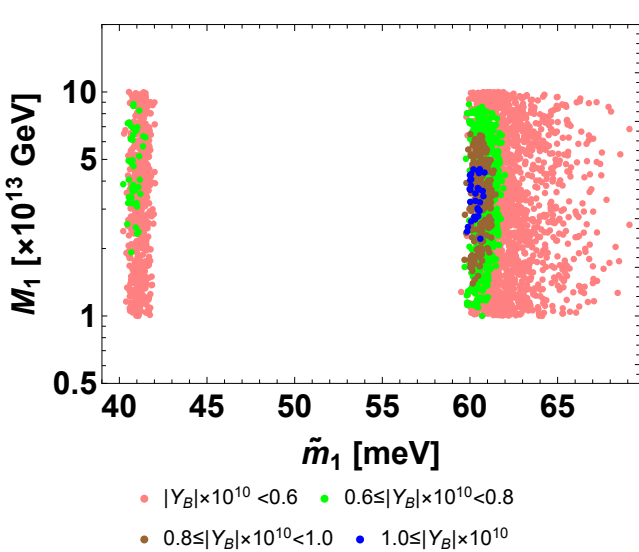


Figure 11: Plot of \tilde{m}_1 and M_1 for each $|Y_B|$.

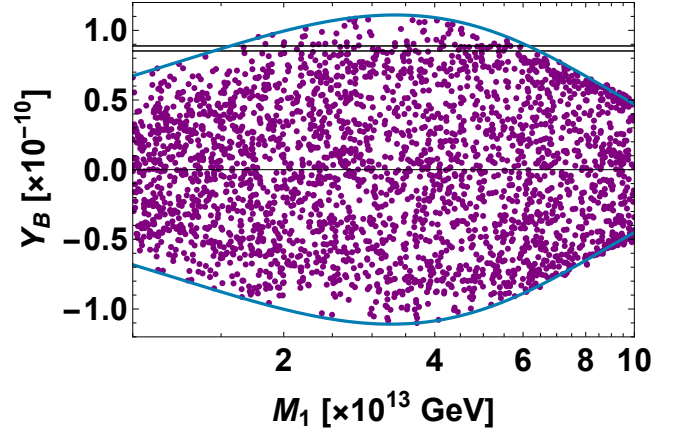


Figure 12: Predictive Y_B versus M_1 . Points correspond to the output of section 4 at $\sqrt{\chi^2} \leq 3$. Horizontal lines denote the upper and lower bounds of observed Y_B in Eq. (39). The blue solid curves denote the boundary of Y_B .

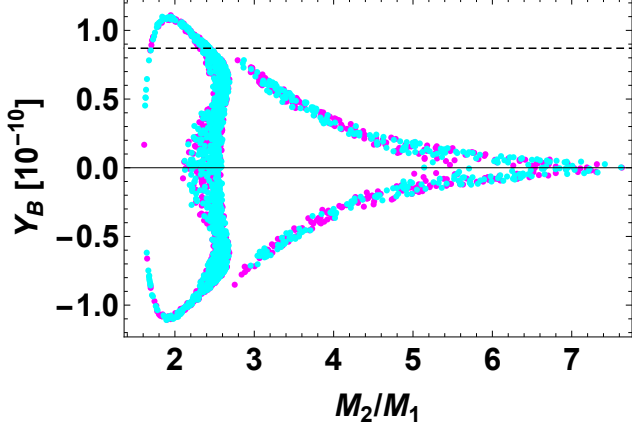


Figure 13: Predictive Y_B versus the mass ratio M_2/M_1 at $M_1 = 3.36 \times 10^{13}$ GeV. Points correspond to the low energy output of section 4 at $\sqrt{\chi^2} \leq 3$, where cyan and magenta correspond to positive and negative $\text{Re}[\tau]$, respectively. Horizontal dashed line denotes the central value of observed Y_B .

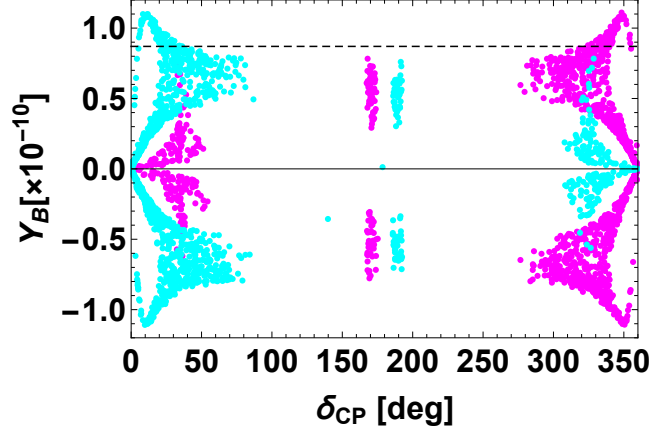


Figure 14: Predictive Y_B versus δ_{CP} at $M_1 = 3.36 \times 10^{13}$ GeV. Points correspond to the low energy output of section 4 at $\sqrt{\chi^2} \leq 3$, where cyan and magenta correspond to positive and negative $\text{Re}[\tau]$, respectively. Horizontal dashed line denotes the central value of observed Y_B .

In order to see which parameter causes the predictive broad Y_B of Fig. 12, we show the M_2/M_1 dependence of Y_B at $M_1 = 3.36 \times 10^{13}$ GeV in Fig. 13. It is clearly found that the predictive magnitude of Y_B depends on M_2/M_1 crucially in addition to the magnitude of M_1 . If M_2/M_1 is fixed in $[1.6, 2]$, the predictive Y_B is in the narrow range, which is consistent with the observed one. However, the present neutrino oscillation data still allow the range $M_2/M_1 = [1.6, 7.6]$ because of the broad τ region in Fig. 1.

Finally, we present Y_B versus δ_{CP} at $M_1 = 3.36 \times 10^{13}$ GeV to see the correlation between the predictive Y_B and the low energy CP violating measure δ_{CP} in Fig. 14. As seen in Fig. 2, there are six regions for the predictive δ_{CP} versus $\text{Re}[\tau]$. Among them, only two regions are available to reproduce the observed BAU. As seen in Fig. 14, the predictive δ_{CP} ranges of $[0^\circ, 50^\circ]$ and $[170^\circ, 175^\circ]$ ($\text{Re}[\tau] < 0$, magenta) cannot reach the observed Y_B , and also $[185^\circ, 190^\circ]$ and $[310^\circ, 360^\circ]$ ($\text{Re}[\tau] > 0$, cyan) cannot reach it, but $[5^\circ, 40^\circ]$ ($\text{Re}[\tau] > 0$, cyan) and $[320^\circ, 355^\circ]$ ($\text{Re}[\tau] < 0$, magenta) attain to the observed Y_B . In these regions, the sum of neutrino masses $\sum m_i$ are expected to be $[66, 84]$ meV, which is read from the output in Fig. 3. In conclusion, the precise determination of the Dirac CP phase δ_{CP} and the sum of neutrino masses $\sum m_i$ will test our model in the future.

We have discussed the leptogenesis in the model of weights ($k_e = -1$, $k_\mu = -3$, $k_\tau = -5$) for right-handed charged leptons. Actually, we have also examined the case of other alternative weights in Appendix D. For the case of ($k_e = -1$, $k_\mu = -1$, $k_\tau = -5$), the predictive Y_B is marginal to reproduce the observed one. On the other hand, the CP asymmetry parameter ε_I of Eq. (40) is much smaller than the above result in the cases of ($k_e = -1$, $k_\mu = -1$, $k_\tau = -7$) and ($k_e = -1$, $k_\mu = -3$, $k_\tau = -7$). Thus, the leptogenesis provides a crucial test to select the favorable models of leptons.

7 Summary

We have presented A_4 modular invariant flavor models of leptons with the CP invariance. The origin of the CP violation is only in the modulus τ . Both CP and modular symmetries are broken spontaneously by the VEV of the modulus τ . We have discussed the phenomenological implication of this model, that is flavor mixing angles and CP violating phases.

We have found allowed region of τ which is consistent with the observed lepton mixing angles and lepton masses for NH at $\sqrt{\chi^2} \leq 3$. The CP violating Dirac phase δ_{CP} is predicted in $[0^\circ, 50^\circ]$, $[170^\circ, 175^\circ]$ and $[280^\circ, 360^\circ]$ for $\text{Re}[\tau] < 0$, and $[0^\circ, 80^\circ]$, $[185^\circ, 190^\circ]$ and $[310^\circ, 360^\circ]$ for $\text{Re}[\tau] > 0$.

The predicted $\sum m_i$ is in $[60, 84]$ meV. By using the predicted Dirac phase and the Majorana phases, we have obtained the effective mass $\langle m_{ee} \rangle$ for the $0\nu\beta\beta$ decay, which is in $[0.003, 3]$ meV.

We have also studied the case of IH of neutrino masses. There are no parameter sets which reproduce the observed masses and three mixing angles below $\sqrt{\chi^2} = 4$. but we have found parameter sets at $\sqrt{\chi^2} = 4-5$.

Our CP invariant lepton mass matrices have minimum number of parameters, eight, apart from the overall scale by putting weights $(k_e = -1, k_\mu = -3, k_\tau = -5)$ for right-handed charged leptons. However, this choice for weights is not a unique one. We have examined alternative three choices: $(k_e = -1, k_\mu = -1, k_\tau = -5)$, $(k_e = -1, k_\mu = -1, k_\tau = -7)$ and $(k_e = -1, k_\mu = -3, k_\tau = -7)$. In those three models, we have also obtained successful numerical results.

The modulus τ links the Dirac CP phase to the baryon asymmetry. We have studied the leptogenesis in our model with NH of neutrino masses. The sign of the BAU is determined by the signs of both $\text{Re}[\tau]$ and g_D . In order to obtain the observed positive Y_B , $(\text{Re}[\tau] < 0, g_D < 0)$ or $(\text{Re}[\tau] > 0, g_D > 0)$ is required. Due to the strong wash-out effect, the yield can be at most the same order of the observed value of the BAU. Then, the lightest right-handed neutrino is in the restricted range $M_1 = [1.5, 6.5] \times 10^{13}$ GeV. In addition, the predictive Y_B also depends on M_2/M_1 crucially.

We have found the correlation between the predictive Y_B and the low energy CP violating measure δ_{CP} . Among six regions of the predictive δ_{CP} versus $\text{Re}[\tau]$, only two ranges of $[5^\circ, 40^\circ]$ ($\text{Re}[\tau] > 0$) and $[320^\circ, 355^\circ]$ ($\text{Re}[\tau] < 0$) are consistent with the BAU, where the sum of neutrino masses $\sum m_i$ is $[66, 84]$ meV.

Thus, our scheme of the modulus τ linking the Dirac CP phase to the baryon asymmetry gives rise to the idea for an important test of the phase relevant to leptogenesis.

Acknowledgments

This research of H.O. was supported by an appointment to the JRG Program at the APCTP through the Science and Technology Promotion Fund and Lottery Fund of the Korean Government. This was also supported by the Korean Local Governments - Gyeongsangbuk-do Province and Pohang City (H.O.). The work of T.Y. was supported by JSPS KAKENHI Grant Numbers 20H01898. H.O. is sincerely grateful for the KIAS member.

Appendix

A Tensor product of A_4 group

We take the generators of A_4 group for the triplet in the symmetric base as follows:

$$S = \frac{1}{3} \begin{pmatrix} -1 & 2 & 2 \\ 2 & -1 & 2 \\ 2 & 2 & -1 \end{pmatrix}, \quad T = \begin{pmatrix} 1 & 0 & 0 \\ 0 & \omega & 0 \\ 0 & 0 & \omega^2 \end{pmatrix}, \quad (43)$$

where $\omega = e^{i\frac{2}{3}\pi}$ for a triplet. In this base, the multiplication rule is

$$\begin{aligned} \begin{pmatrix} a_1 \\ a_2 \\ a_3 \end{pmatrix}_{\mathbf{3}} \otimes \begin{pmatrix} b_1 \\ b_2 \\ b_3 \end{pmatrix}_{\mathbf{3}} &= (a_1b_1 + a_2b_3 + a_3b_2)_{\mathbf{1}} \oplus (a_3b_3 + a_1b_2 + a_2b_1)_{\mathbf{1}'} \\ &\oplus (a_2b_2 + a_1b_3 + a_3b_1)_{\mathbf{1}''} \\ &\oplus \frac{1}{3} \begin{pmatrix} 2a_1b_1 - a_2b_3 - a_3b_2 \\ 2a_3b_3 - a_1b_2 - a_2b_1 \\ 2a_2b_2 - a_1b_3 - a_3b_1 \end{pmatrix}_{\mathbf{3}} \oplus \frac{1}{2} \begin{pmatrix} a_2b_3 - a_3b_2 \\ a_1b_2 - a_2b_1 \\ a_3b_1 - a_1b_3 \end{pmatrix}_{\mathbf{3}}, \end{aligned}$$

$$\mathbf{1} \otimes \mathbf{1} = \mathbf{1}, \quad \mathbf{1}' \otimes \mathbf{1}' = \mathbf{1}'' , \quad \mathbf{1}'' \otimes \mathbf{1}'' = \mathbf{1}' , \quad \mathbf{1}' \otimes \mathbf{1}'' = \mathbf{1}, \quad (44)$$

where

$$T(\mathbf{1}') = \omega, \quad T(\mathbf{1}'') = \omega^2. \quad (45)$$

More details are shown in the review [6, 7].

B Modular forms in A_4 symmetry

For $\Gamma_3 \simeq A_4$, the dimension of the linear space $\mathcal{M}_k(\Gamma(3))$ of modular forms of weight k is $k + 1$ [128–130], i.e., there are three linearly independent modular forms of the lowest non-trivial weight 2. These forms have been explicitly obtained [22] in terms of the Dedekind eta-function $\eta(\tau)$:

$$\eta(\tau) = q^{1/24} \prod_{n=1}^{\infty} (1 - q^n), \quad q = \exp(i2\pi\tau), \quad (46)$$

where $\eta(\tau)$ is a so-called modular form of weight 1/2. We use the base of the generators S and T in Eq. (43) for the triplet representation. Then, the modular forms of weight 2 ($k = 2$) transforming as a triplet of A_4 , $Y_{\mathbf{3}}^{(2)}(\tau) = (Y_1(\tau), Y_2(\tau), Y_3(\tau))^T$, can be written in terms of $\eta(\tau)$ and its derivative [22]:

$$\begin{aligned} Y_1(\tau) &= \frac{i}{2\pi} \left(\frac{\eta'(\tau/3)}{\eta(\tau/3)} + \frac{\eta'((\tau+1)/3)}{\eta((\tau+1)/3)} + \frac{\eta'((\tau+2)/3)}{\eta((\tau+2)/3)} - \frac{27\eta'(3\tau)}{\eta(3\tau)} \right), \\ Y_2(\tau) &= \frac{-i}{\pi} \left(\frac{\eta'(\tau/3)}{\eta(\tau/3)} + \omega^2 \frac{\eta'((\tau+1)/3)}{\eta((\tau+1)/3)} + \omega \frac{\eta'((\tau+2)/3)}{\eta((\tau+2)/3)} \right), \\ Y_3(\tau) &= \frac{-i}{\pi} \left(\frac{\eta'(\tau/3)}{\eta(\tau/3)} + \omega \frac{\eta'((\tau+1)/3)}{\eta((\tau+1)/3)} + \omega^2 \frac{\eta'((\tau+2)/3)}{\eta((\tau+2)/3)} \right). \end{aligned} \quad (47)$$

The overall coefficient in Eq. (47) is one possible choice. It cannot be uniquely determined. The triplet modular forms of weight 2 have the following q -expansions:

$$Y_{\mathbf{3}}^{(2)}(\tau) = \begin{pmatrix} Y_1(\tau) \\ Y_2(\tau) \\ Y_3(\tau) \end{pmatrix} = \begin{pmatrix} 1 + 12q + 36q^2 + 12q^3 + \dots \\ -6q^{1/3}(1 + 7q + 8q^2 + \dots) \\ -18q^{2/3}(1 + 2q + 5q^2 + \dots) \end{pmatrix}. \quad (48)$$

They satisfy also the constraint [22]:

$$Y_2(\tau)^2 + 2Y_1(\tau)Y_3(\tau) = 0. \quad (49)$$

The modular forms of the higher weight, k , can be obtained by using the A_4 tensor products of Appendix A in terms of the modular forms with weight 2, $Y_{\mathbf{3}}^{(2)}(\tau)$.

C Majorana and Dirac phases and $\langle m_{ee} \rangle$ in $0\nu\beta\beta$ decay

Supposing neutrinos to be Majorana particles, the PMNS matrix U_{PMNS} [118, 119] is parametrized in terms of the three mixing angles θ_{ij} ($i, j = 1, 2, 3$; $i < j$), one CP violating Dirac phase δ_{CP} and two Majorana phases α_{21} , α_{31} as follows:

$$U_{\text{PMNS}} = \begin{pmatrix} c_{12}c_{13} & s_{12}c_{13} & s_{13}e^{-i\delta_{\text{CP}}} \\ -s_{12}c_{23} - c_{12}s_{23}s_{13}e^{i\delta_{\text{CP}}} & c_{12}c_{23} - s_{12}s_{23}s_{13}e^{i\delta_{\text{CP}}} & s_{23}c_{13} \\ s_{12}s_{23} - c_{12}c_{23}s_{13}e^{i\delta_{\text{CP}}} & -c_{12}s_{23} - s_{12}c_{23}s_{13}e^{i\delta_{\text{CP}}} & c_{23}c_{13} \end{pmatrix} \begin{pmatrix} 1 & 0 & 0 \\ 0 & e^{i\frac{\alpha_{21}}{2}} & 0 \\ 0 & 0 & e^{i\frac{\alpha_{31}}{2}} \end{pmatrix}, \quad (50)$$

where c_{ij} and s_{ij} denote $\cos\theta_{ij}$ and $\sin\theta_{ij}$, respectively.

The rephasing invariant CP violating measure of leptons [148, 149] is defined by the PMNS matrix elements $U_{\alpha i}$. It is written in terms of the mixing angles and the CP violating phase as:

$$J_{CP} = \text{Im} [U_{e1}U_{\mu 2}U_{e2}^*U_{\mu 1}^*] = s_{23}c_{23}s_{12}c_{12}s_{13}c_{13}^2 \sin \delta_{\text{CP}}, \quad (51)$$

where $U_{\alpha i}$ denotes the each component of the PMNS matrix.

There are also other invariants I_1 and I_2 associated with Majorana phases

$$I_1 = \text{Im} [U_{e1}^*U_{e2}] = c_{12}s_{12}c_{13}^2 \sin \left(\frac{\alpha_{21}}{2} \right), \quad I_2 = \text{Im} [U_{e1}^*U_{e3}] = c_{12}s_{13}c_{13} \sin \left(\frac{\alpha_{31}}{2} - \delta_{\text{CP}} \right). \quad (52)$$

We can calculate δ_{CP} , α_{21} and α_{31} with these relations by taking account of

$$\begin{aligned} \cos \delta_{CP} &= \frac{|U_{\tau 1}|^2 - s_{12}^2 s_{23}^2 - c_{12}^2 c_{23}^2 s_{13}^2}{2c_{12}s_{12}c_{23}s_{23}s_{13}}, \\ \text{Re} [U_{e1}^*U_{e2}] &= c_{12}s_{12}c_{13}^2 \cos \left(\frac{\alpha_{21}}{2} \right), \quad \text{Re} [U_{e1}^*U_{e3}] = c_{12}s_{13}c_{13} \cos \left(\frac{\alpha_{31}}{2} - \delta_{\text{CP}} \right). \end{aligned} \quad (53)$$

In terms of this parametrization, the effective mass for the $0\nu\beta\beta$ decay is given as follows:

$$\langle m_{ee} \rangle = |m_1 c_{12}^2 c_{13}^2 + m_2 s_{12}^2 c_{13}^2 e^{i\alpha_{21}} + m_3 s_{13}^2 e^{i(\alpha_{31} - 2\delta_{CP})}|. \quad (54)$$

D Alternative A_4 modular models

We present three alternative charged lepton mass matrices by putting different weights for (k_e, k_μ, k_τ) , which are consistent with observed mixing angles and masses. Neutrino mass matrix is the same one in section 3.

D.1 Case of $(k_e = -1, k_\mu = -1, k_\tau = -5)$ for charged leptons

The assignment of MSSM fields and modular forms are given in Table 4.

	L	(e^c, μ^c, τ^c)	N^c	H_u	H_d	$Y_{\mathbf{3}}^{(2)}, Y_{\mathbf{r}}^{(6)}$
$SU(2)$	2	1	1	2	2	1
A_4	3	(1, 1'', 1')	3	1	1	3, {3, 3'}
k	-1	(-1, -3, -5)	-1	0	0	2, 6

Table 4: Representations and weights k for MSSM fields and modular forms of weights 2 and 6.

The A_4 invariant superpotential of the charged leptons, w_E , by taking into account the modular weights is obtained as

$$w_E = \alpha_e e^c H_d Y_{\mathbf{3}}^{(2)} L + \beta_e \mu^c H_d Y_{\mathbf{3}}^{(4)} L + \gamma_e \tau^c H_d Y_{\mathbf{3}}^{(6)} L + \gamma'_e \tau^c H_d Y_{\mathbf{3}'}^{(6)} L. \quad (55)$$

By using $g_e = \gamma'_e / \gamma_e$, the charged lepton mass matrix M_E is simply written as:

$$M_E(\tau) = v_d \begin{pmatrix} \alpha_e & 0 & 0 \\ 0 & \beta_e & 0 \\ 0 & 0 & \gamma_e \end{pmatrix} \begin{pmatrix} Y_1(\tau) & Y_3(\tau) & Y_2(\tau) \\ Y_2(\tau) & Y_1(\tau) & Y_3(\tau) \\ Y_{\mathbf{3}}^{(6)}(\tau) + g_e Y_{\mathbf{3}}^{\prime(6)}(\tau) & Y_2^{(6)}(\tau) + g_e Y_2^{\prime(6)}(\tau) & Y_1^{(6)}(\tau) + g_e Y_1^{\prime(6)}(\tau) \end{pmatrix}_{RL}. \quad (56)$$

D.2 Case of $(k_e = -1, k_\mu = -1, k_\tau = -7)$ for charged leptons

The assignment of MSSM fields and modular forms are given in Table 5.

	L	(e^c, μ^c, τ^c)	N^c	H_u	H_d	$Y_{\mathbf{3}}^{(2)}, Y_{\mathbf{r}}^{(8)}$
$SU(2)$	2	1	1	2	2	1
A_4	3	(1, 1'', 1')	3	1	1	3, {3, 3'}
k	-1	(-1, -1, -7)	-1	0	0	2, 8

Table 5: Representations and weights k for MSSM fields and modular forms of weights 2 and 8.

For $k = 8$, there are 9 modular forms by the tensor products of A_4 as:

$$Y_1^{(8)} = (Y_1^2 + 2Y_2Y_3)^2, \quad Y_{1'}^{(8)} = (Y_1^2 + 2Y_2Y_3)(Y_3^2 + 2Y_1Y_2), \quad Y_{1''}^{(8)} = (Y_3^2 + 2Y_1Y_2)^2, \\ Y_{\mathbf{3}}^{(8)} \equiv \begin{pmatrix} Y_1^{(8)} \\ Y_2^{(8)} \\ Y_3^{(8)} \end{pmatrix} = (Y_1^3 + Y_2^3 + Y_3^3 - 3Y_1Y_2Y_3) \begin{pmatrix} Y_1 \\ Y_2 \\ Y_3 \end{pmatrix}, \quad Y_{\mathbf{3}'}^{(8)} \equiv \begin{pmatrix} Y_1^{\prime(8)} \\ Y_2^{\prime(8)} \\ Y_3^{\prime(8)} \end{pmatrix} = (Y_3^2 + 2Y_1Y_2) \begin{pmatrix} Y_2^2 - Y_1Y_3 \\ Y_1^2 - Y_2Y_3 \\ Y_3^2 - Y_1Y_2 \end{pmatrix}.$$

The A_4 invariant superpotential of the charged leptons, w_E , by taking into account the modular weights is obtained as

$$w_E = \alpha_e e^c H_d Y_{\mathbf{3}}^{(2)} L + \beta_e \mu^c H_d Y_{\mathbf{3}}^{(2)} L + \gamma_e \tau^c H_d Y_{\mathbf{3}}^{(8)} L + \gamma'_e \tau^c H_d Y_{\mathbf{3}'}^{(8)} L. \quad (57)$$

By using $g_e = \gamma'_e/\gamma_e$, the charged lepton mass matrix M_E is simply written as:

$$M_E(\tau) = v_d \begin{pmatrix} \alpha_e & 0 & 0 \\ 0 & \beta_e & 0 \\ 0 & 0 & \gamma_e \end{pmatrix} \begin{pmatrix} Y_1(\tau) & Y_3(\tau) & Y_2(\tau) \\ Y_2(\tau) & Y_1(\tau) & Y_3(\tau) \\ Y_3^{(8)}(\tau) + g_e Y_3'^{(8)}(\tau) & Y_2^{(8)}(\tau) + g_e Y_2'^{(8)}(\tau) & Y_1^{(8)}(\tau) + g_e Y_1'^{(8)}(\tau) \end{pmatrix}_{RL}. \quad (58)$$

D.3 Case of $(k_e = -1, k_\mu = -3, k_\tau = -7)$ for charged leptons

The assignment of MSSM fields and modular forms are given in Table 6.

	L	(e^c, μ^c, τ^c)	N^c	H_u	H_d	$Y_{\mathbf{3}}^{(2)}, Y_{\mathbf{3}}^{(4)}, Y_{\mathbf{r}}^{(8)}$
$SU(2)$	2	1	1	2	2	1
A_4	3	(1, 1'', 1')	3	1	1	3, 3, {3, 3'}
k	-1	(-1, -3, -7)	-1	0	0	2, 4, 8

Table 6: Representations and weights k for MSSM fields and modular forms of weights 2, 4 and 8.

The A_4 invariant superpotential of the charged leptons, w_E , by taking into account the modular weights is obtained as

$$w_E = \alpha_e e^c H_d Y_{\mathbf{3}}^{(2)} L + \beta_e \mu^c H_d Y_{\mathbf{3}}^{(4)} L + \gamma_e \tau^c H_d Y_{\mathbf{3}}^{(8)} L + \gamma'_e \tau^c H_d Y_{\mathbf{3}'}^{(8)} L. \quad (59)$$

By using $g_e = \gamma'_e/\gamma_e$, the charged lepton mass matrix M_E is simply written as:

$$M_E(\tau) = v_d \begin{pmatrix} \alpha_e & 0 & 0 \\ 0 & \beta_e & 0 \\ 0 & 0 & \gamma_e \end{pmatrix} \begin{pmatrix} Y_1(\tau) & Y_3(\tau) & Y_2(\tau) \\ Y_2^{(4)}(\tau) & Y_1^{(4)}(\tau) & Y_3^{(4)}(\tau) \\ Y_3^{(8)}(\tau) + g_e Y_3'^{(8)}(\tau) & Y_2^{(8)}(\tau) + g_e Y_2'^{(8)}(\tau) & Y_1^{(8)}(\tau) + g_e Y_1'^{(8)}(\tau) \end{pmatrix}_{RL}. \quad (60)$$

D.4 Sample parameters of alternative models

In Table 7, we show parameters and output of our calculations in above three cases of (k_e, k_μ, k_τ) for NH.

(k_e, k_μ, k_τ)	$(-1, -1, -5)$	$(-1, -1, -7)$	$(-1, -3, -7)$
τ	$-0.1912 + 1.1194 i$	$0.0901 + 1.0047 i$	$-0.1027 + 1.0050 i$
g_D	-0.800	-0.660	0.685
g_e	-0.905	-0.530	-0.573
β_e/α_e	3.70×10^{-3}	5.94×10^{-3}	6.30×10^{-3}
γ_e/α_e	9.71	17.6	16.0
$\sin^2 \theta_{12}$	0.305	0.324	0.326
$\sin^2 \theta_{23}$	0.569	0.441	0.479
$\sin^2 \theta_{13}$	0.0222	0.0222	0.0223
δ_{CP}^ℓ	172°	183°	176°
$[\alpha_{21}, \alpha_{31}]$	$[192^\circ, 263^\circ]$	$[181^\circ, -0.1^\circ]$	$[179^\circ, 0.2^\circ]$
$\sum m_i$	62.5 meV	60.5 meV	60.7 meV
$\langle m_{ee} \rangle$	1.69 meV	0.58 meV	0.52 meV
$\sqrt{\chi^2}$	1.08	2.16	2.38

Table 7: Numerical values of parameters and observables at sample points of NH.

E Formulae of the leptogenesis

We solve the Boltzmann equations for right-handed neutrinos number densities n_{N_I} and the lepton asymmetry density n_L as:

$$\frac{dY_{N_I}}{dz} = \frac{-z}{sH(M_1)} \left\{ \left(\frac{Y_{N_I}}{Y_{N_I}^{eq}} - 1 \right) \left(\gamma_{N_I} + 2\gamma_{tI}^{(3)} + 4\gamma_{tI}^{(4)} \right) + \sum_{J=1}^3 \left(\frac{Y_{N_I} Y_{N_J}}{Y_{N_I}^{eq} Y_{N_J}^{eq}} - 1 \right) \left(\gamma_{N_I N_J}^{(2)} + \gamma_{N_I N_J}^{(3)} \right) \right\}, \quad (61)$$

$$\begin{aligned} \frac{dY_L}{dz} = \frac{-z}{sH(M_1)} \left\{ \sum_{I=1}^3 \left[\left(1 - \frac{Y_{N_I}}{Y_{N_I}^{eq}} \right) \varepsilon_I \gamma_{N_I} + \frac{Y_L}{Y_\ell^{eq}} \frac{\gamma_{N_I}}{2} \right] + \frac{Y_L}{Y_\ell^{eq}} \left(2\gamma_N^{(2)} + 2\gamma_N^{(13)} \right) \right. \\ \left. + \frac{Y_L}{Y_\ell^{eq}} \sum_{I=1}^3 \left[\frac{Y_{N_I}}{Y_{N_I}^{eq}} \gamma_{tI}^{(3)} + 2\gamma_{tI}^{(4)} + \frac{Y_{N_I}}{Y_{N_I}^{eq}} \left(\gamma_{WI}^{(1)} + \gamma_{BI}^{(1)} \right) + \gamma_{WI}^{(2)} + \gamma_{WI}^{(3)} + \gamma_{BI}^{(2)} + \gamma_{BI}^{(3)} \right] \right\}, \quad (62) \end{aligned}$$

where $z = M_1/T$. Here we define the yields as $Y_{N_I} = n_{N_I}/s$ and $Y_L = n_L/s$, with the entropy density of the universe s . The superscript "eq" denotes its equilibrium value. We apply the Boltzmann approximation and the yield for a massless particle with one degree of freedom in equilibrium is given by $Y_\ell^{eq} = 45/(2\pi^4 g_{*s})$, with $g_{*s} = 110.75$.

The flavor summed CP asymmetry at the decay of the right-handed neutrino N_I is given as

$$\varepsilon_I = -\frac{1}{8\pi} \sum_{J \neq I} \frac{\text{Im}[\{(y_\nu y_\nu^\dagger)_{IJ}\}^2]}{(y_\nu y_\nu^\dagger)_{II}} \left[f^V \left(\frac{M_J^2}{M_I^2} \right) + f^S \left(\frac{M_J^2}{M_I^2} \right) \right], \quad (63)$$

where $f^V(x)$ and $f^S(x)$ are the contributions from vertex and self-energy corrections, respectively.

In the case of the standard model (SM) with right-handed neutrinos, they are given as

$$f^V(x) = \sqrt{x} \left[(x+1) \ln \left(1 + \frac{1}{x} \right) - 1 \right], \quad f^S(x) = \frac{\sqrt{x}}{x-1}. \quad (64)$$

The reaction density for the N_I decay is given by

$$\gamma_{N_I} = \frac{(y_\nu y_\nu^\dagger)_{II}}{8\pi^3} M_1^4 a_I^{3/2} \frac{K_1(\sqrt{a_I} z)}{z}, \quad (65)$$

where $z = M_1/T$, $a_I = (M_I/M_1)^2$, and $K_1(x)$ is the modified Bessel function of the second kind. Note that y_ν is the Yukawa coupling matrix of neutrinos in the base where both the mass matrices of charged leptons and right-handed neutrinos are diagonalized. The reaction density for the scattering process $A + B \rightarrow C + D$ is expressed as

$$\gamma(A + B \rightarrow C + D) = \frac{T}{64\pi^4} \int_{(m_A+m_B)^2}^{\infty} ds \hat{\sigma}(s) \sqrt{s} K_1\left(\frac{\sqrt{s}}{T}\right), \quad (66)$$

where m_A and m_B are masses of the initial particles and $\hat{\sigma}(s)$ denotes the reduced cross section for the process. The expressions of the reduced cross sections for the $\Delta L = 1$ processes induced through top Yukawa interaction, the $\Delta L = 2$ scattering processes and the annihilation processes of right-handed neutrinos are found in Ref. [150]. The reduced cross section for $L\bar{H}_u \rightarrow \bar{L}H_u$ process which is correctly subtracted N_I on-shell contribution is [151]

$$\begin{aligned} \hat{\sigma}_N^{(2)}(x) = & \frac{1}{2\pi} \left[\sum_I (y_\nu y_\nu^\dagger)_{II}^2 \frac{a_I}{x} \left\{ \frac{x}{a_I} + \frac{x}{D_I} - \left(1 + \frac{x+a_I}{D_I} \right) \log \left(\frac{x+a_I}{a_I} \right) \right\} \right. \\ & + \sum_{I>J} \text{Re}[(y_\nu y_\nu^\dagger)_{IJ}^2] \frac{\sqrt{a_I a_J}}{x} \left\{ \frac{x^2 + x(D_I + D_J)}{D_I D_J} + (x+a_I) \left(\frac{2}{a_J - a_I} - \frac{1}{D_J} \right) \ln \left(\frac{x+a_I}{a_I} \right) \right. \\ & \left. \left. + (x+a_J) \left(\frac{2}{a_I - a_J} - \frac{1}{D_I} \right) \ln \left(\frac{x+a_J}{a_J} \right) \right\} \right], \quad (67) \end{aligned}$$

where $D_I = [(x - a_I)^2 + a_I c_I]/(x - a_I)$ with $c_I = (\Gamma_{N_I}/M_1)^2$, in which Γ_{N_I} is the total decay rate of right-handed neutrino N_I . The explicit form of reduced cross sections for $\Delta L = 1$ processes through the $SU(2)_L$ SM gauge interaction are found in Refs. [136, 151],

$$\begin{aligned} \hat{\sigma}_{WI}^{(1)}(x) = & \frac{3g_2^2 (y_\nu y_\nu^\dagger)_{II}}{16\pi x^2} \left[-2x^2 + 6a_I x - 4a_I^2 + (x^2 - 2a_I x + 2a_I^2) \ln \left| \frac{x - a_I + a_L}{a_L} \right| \right. \\ & \left. + \frac{x(a_L x + a_L a_I - a_W a_I)(a_I - x)}{a_L(x - a_I + a_L)} \right], \quad (68) \end{aligned}$$

$$\hat{\sigma}_{WI}^{(2)}(x) = \frac{3g_2^2 (y_\nu y_\nu^\dagger)_{II}}{8\pi x(x - a_I)} \left[2a_I x \ln \left| \frac{x - a_I + a_H}{a_H} \right| + (x^2 + a_I^2) \ln \left| \frac{x - a_I - a_W - a_H}{-a_W - a_H} \right| \right], \quad (69)$$

$$\hat{\sigma}_{WI}^{(3)}(x) = \frac{3g_2^2 (y_\nu y_\nu^\dagger)_{II} a_I}{16\pi x^2} \left[\frac{x^2 - 4a_I x + 3a_I^2}{a_I} + 4(x - a_I) \ln \left| \frac{x - a_I + a_H}{a_H} \right| - \frac{x(4a_H - a_W)(x - a_I)}{a_H(x - a_I + m_H)} \right]. \quad (70)$$

Here $\hat{\sigma}_{WI}^{(1)}$, $\hat{\sigma}_{WI}^{(2)}$ and $\hat{\sigma}_{WI}^{(3)}$ correspond to the reduced cross sections of the processes $N_I L \rightarrow H_u W$, $N_I W \rightarrow \bar{L} H_u$ and $N_I \bar{H}_u \rightarrow \bar{L} W$, respectively. We have used $a_X = m_X^2/M_1^2$ where m_X with $X = L, H_u, W, B$ are thermal masses of lepton doublets, up-type Higgs, $SU(2)_L$ gauge bosons and $U(1)_Y$ gauge boson, respectively. The reaction densities for the $\Delta L = 1$ processes through $U(1)_Y$ gauge interaction $\hat{\sigma}_{BI}^{(i)}$ are obtained by replacing a_W with a_B and $\frac{3}{2}g_2^2$ with $\frac{1}{4}g_Y^2$ in $\hat{\sigma}_{WI}^{(i)}$.

For the more accurate estimation of the baryon asymmetry, we have taken into account the one-loop RGE evolutions of couplings and the renormalization scale is taken as $\mu = 2\pi T$.

References

- [1] M. Fukugita, M. Tanimoto and T. Yanagida, Phys. Rev. D **57** (1998) 4429 [hep-ph/9709388].
- [2] Y. Fukuda *et al.* [Super-Kamiokande Collaboration], Phys. Rev. Lett. **81** (1998) 1562 [hep-ex/9807003].
- [3] F. Wilczek and A. Zee, Phys. Lett. **70B** (1977) 418 Erratum: [Phys. Lett. **72B** (1978) 504].
- [4] S. Pakvasa and H. Sugawara, Phys. Lett. **73B** (1978) 61.
- [5] G. Altarelli and F. Feruglio, Rev. Mod. Phys. **82** (2010) 2701 [arXiv:1002.0211 [hep-ph]].
- [6] H. Ishimori, T. Kobayashi, H. Ohki, Y. Shimizu, H. Okada and M. Tanimoto, Prog. Theor. Phys. Suppl. **183** (2010) 1 [arXiv:1003.3552 [hep-th]].
- [7] H. Ishimori, T. Kobayashi, H. Ohki, H. Okada, Y. Shimizu and M. Tanimoto, Lect. Notes Phys. **858** (2012) 1, Springer.
- [8] D. Hernandez and A. Y. Smirnov, Phys. Rev. D **86** (2012) 053014 [arXiv:1204.0445 [hep-ph]].
- [9] S. F. King and C. Luhn, Rept. Prog. Phys. **76** (2013) 056201 [arXiv:1301.1340 [hep-ph]].
- [10] S. F. King, A. Merle, S. Morisi, Y. Shimizu and M. Tanimoto, New J. Phys. **16**, 045018 (2014) [arXiv:1402.4271 [hep-ph]].
- [11] M. Tanimoto, AIP Conf. Proc. **1666** (2015) 120002.
- [12] S. F. King, Prog. Part. Nucl. Phys. **94** (2017) 217 [arXiv:1701.04413 [hep-ph]].
- [13] S. T. Petcov, Eur. Phys. J. C **78** (2018) no.9, 709 [arXiv:1711.10806 [hep-ph]].
- [14] F. Feruglio and A. Romanino, arXiv:1912.06028 [hep-ph].
- [15] E. Ma and G. Rajasekaran, Phys. Rev. D **64**, 113012 (2001) [arXiv:hep-ph/0106291].
- [16] K. S. Babu, E. Ma and J. W. F. Valle, Phys. Lett. B **552**, 207 (2003) [arXiv:hep-ph/0206292].
- [17] G. Altarelli and F. Feruglio, Nucl. Phys. B **720** (2005) 64 [hep-ph/0504165].
- [18] G. Altarelli and F. Feruglio, Nucl. Phys. B **741** (2006) 215 [hep-ph/0512103].

- [19] Y. Shimizu, M. Tanimoto and A. Watanabe, *Prog. Theor. Phys.* **126** (2011) 81 [arXiv:1105.2929 [hep-ph]].
- [20] S. T. Petcov and A. V. Titov, *Phys. Rev. D* **97** (2018) no.11, 115045 [arXiv:1804.00182 [hep-ph]].
- [21] S. K. Kang, Y. Shimizu, K. Takagi, S. Takahashi and M. Tanimoto, *PTEP* **2018**, no. 8, 083B01 (2018) [arXiv:1804.10468 [hep-ph]].
- [22] F. Feruglio, in *From My Vast Repertoire ...: Guido Altarelli's Legacy*, A. Levy, S. Forte, Stefano, and G. Ridolfi, eds., pp.227–266, 2019, arXiv:1706.08749 [hep-ph].
- [23] R. de Adelhart Toorop, F. Feruglio and C. Hagedorn, *Nucl. Phys. B* **858**, 437 (2012) [arXiv:1112.1340 [hep-ph]].
- [24] T. Kobayashi, K. Tanaka and T. H. Tatsuishi, *Phys. Rev. D* **98** (2018) no.1, 016004 [arXiv:1803.10391 [hep-ph]].
- [25] J. T. Penedo and S. T. Petcov, *Nucl. Phys. B* **939** (2019) 292 [arXiv:1806.11040 [hep-ph]].
- [26] P. P. Novichkov, J. T. Penedo, S. T. Petcov and A. V. Titov, *JHEP* **1904** (2019) 174 [arXiv:1812.02158 [hep-ph]].
- [27] J. C. Criado and F. Feruglio, *SciPost Phys.* **5** (2018) no.5, 042 [arXiv:1807.01125 [hep-ph]].
- [28] T. Kobayashi, N. Omoto, Y. Shimizu, K. Takagi, M. Tanimoto and T. H. Tatsuishi, *JHEP* **1811** (2018) 196 [arXiv:1808.03012 [hep-ph]].
- [29] G. J. Ding, S. F. King and X. G. Liu, *JHEP* **1909** (2019) 074 [arXiv:1907.11714 [hep-ph]].
- [30] P. P. Novichkov, J. T. Penedo, S. T. Petcov and A. V. Titov, *JHEP* **1904** (2019) 005 [arXiv:1811.04933 [hep-ph]].
- [31] T. Kobayashi, Y. Shimizu, K. Takagi, M. Tanimoto and T. H. Tatsuishi, *JHEP* **02** (2020), 097 [arXiv:1907.09141 [hep-ph]].
- [32] X. Wang and S. Zhou, *JHEP* **05** (2020), 017 [arXiv:1910.09473 [hep-ph]].
- [33] G. J. Ding, S. F. King and X. G. Liu, *Phys. Rev. D* **100** (2019) no.11, 115005 [arXiv:1903.12588 [hep-ph]].
- [34] X. G. Liu and G. J. Ding, *JHEP* **1908** (2019) 134 [arXiv:1907.01488 [hep-ph]].
- [35] P. Chen, G. J. Ding, J. N. Lu and J. W. F. Valle, *Phys. Rev. D* **102** (2020) no.9, 095014 [arXiv:2003.02734 [hep-ph]].
- [36] P. P. Novichkov, J. T. Penedo and S. T. Petcov, *Nucl. Phys. B* **963** (2021), 115301 [arXiv:2006.03058 [hep-ph]].
- [37] X. G. Liu, C. Y. Yao and G. J. Ding, *Phys. Rev. D* **103** (2021) no.5, 056013 [arXiv:2006.10722 [hep-ph]].

- [38] I. de Medeiros Varzielas, S. F. King and Y. L. Zhou, Phys. Rev. D **101** (2020) no.5, 055033 [arXiv:1906.02208 [hep-ph]].
- [39] G. J. Ding, S. F. King, C. C. Li and Y. L. Zhou, JHEP **08** (2020), 164 [arXiv:2004.12662 [hep-ph]].
- [40] T. Asaka, Y. Heo, T. H. Tatsuishi and T. Yoshida, JHEP **2001** (2020) 144 [arXiv:1909.06520 [hep-ph]].
- [41] T. Asaka, Y. Heo and T. Yoshida, Phys. Lett. B **811** (2020), 135956 [arXiv:2009.12120 [hep-ph]].
- [42] M. K. Behera, S. Mishra, S. Singirala and R. Mohanta, [arXiv:2007.00545 [hep-ph]].
- [43] S. Mishra, [arXiv:2008.02095 [hep-ph]].
- [44] F. J. de Anda, S. F. King and E. Perdomo, Phys. Rev. D **101** (2020) no.1, 015028 [arXiv:1812.05620 [hep-ph]].
- [45] T. Kobayashi, Y. Shimizu, K. Takagi, M. Tanimoto and T. H. Tatsuishi, arXiv:1906.10341 [hep-ph].
- [46] P. P. Novichkov, S. T. Petcov and M. Tanimoto, Phys. Lett. B **793** (2019) 247 [arXiv:1812.11289 [hep-ph]].
- [47] T. Kobayashi, Y. Shimizu, K. Takagi, M. Tanimoto, T. H. Tatsuishi and H. Uchida, Phys. Lett. B **794** (2019) 114 [arXiv:1812.11072 [hep-ph]].
- [48] H. Okada and M. Tanimoto, Phys. Lett. B **791** (2019) 54 [arXiv:1812.09677 [hep-ph]].
- [49] H. Okada and M. Tanimoto, Eur. Phys. J. C **81** (2021) no.1, 52 [arXiv:1905.13421 [hep-ph]].
- [50] T. Nomura and H. Okada, Phys. Lett. B **797** (2019) 134799 [arXiv:1904.03937 [hep-ph]].
- [51] H. Okada and Y. Orikasa, Phys. Rev. D **100** (2019) no.11, 115037 [arXiv:1907.04716 [hep-ph]].
- [52] Y. Kariyazono, T. Kobayashi, S. Takada, S. Tamba and H. Uchida, Phys. Rev. D **100** (2019) no.4, 045014 [arXiv:1904.07546 [hep-th]].
- [53] T. Nomura and H. Okada, Nucl. Phys. B **966** (2021), 115372 [arXiv:1906.03927 [hep-ph]].
- [54] H. Okada and Y. Orikasa, arXiv:1908.08409 [hep-ph].
- [55] T. Nomura, H. Okada and O. Popov, Phys. Lett. B **803** (2020) 135294 [arXiv:1908.07457 [hep-ph]].
- [56] J. C. Criado, F. Feruglio and S. J. D. King, JHEP **2002** (2020) 001 [arXiv:1908.11867 [hep-ph]].
- [57] S. F. King and Y. L. Zhou, Phys. Rev. D **101** (2020) no.1, 015001 [arXiv:1908.02770 [hep-ph]].
- [58] G. J. Ding, S. F. King, X. G. Liu and J. N. Lu, JHEP **1912** (2019) 030 [arXiv:1910.03460 [hep-ph]].

- [59] I. de Medeiros Varzielas, M. Levy and Y. L. Zhou, JHEP **11** (2020), 085 [arXiv:2008.05329 [hep-ph]].
- [60] D. Zhang, Nucl. Phys. B **952** (2020) 114935 [arXiv:1910.07869 [hep-ph]].
- [61] T. Nomura, H. Okada and S. Patra, Nucl. Phys. B **967** (2021), 115395 [arXiv:1912.00379 [hep-ph]].
- [62] T. Kobayashi, T. Nomura and T. Shimomura, Phys. Rev. D **102** (2020) no.3, 035019 [arXiv:1912.00637 [hep-ph]].
- [63] J. N. Lu, X. G. Liu and G. J. Ding, Phys. Rev. D **101** (2020) no.11, 115020 [arXiv:1912.07573 [hep-ph]].
- [64] X. Wang, Nucl. Phys. B **957** (2020), 115105 [arXiv:1912.13284 [hep-ph]].
- [65] S. J. D. King and S. F. King, JHEP **09** (2020), 043 [arXiv:2002.00969 [hep-ph]].
- [66] M. Abbas, Phys. Rev. D **103** (2021) no.5, 056016 [arXiv:2002.01929 [hep-ph]].
- [67] H. Okada and Y. Shoji, Phys. Dark Univ. **31** (2021), 100742 [arXiv:2003.11396 [hep-ph]].
- [68] H. Okada and Y. Shoji, Nucl. Phys. B **961** (2020), 115216 [arXiv:2003.13219 [hep-ph]].
- [69] G. J. Ding and F. Feruglio, JHEP **06** (2020), 134 [arXiv:2003.13448 [hep-ph]].
- [70] T. Nomura and H. Okada, [arXiv:2007.04801 [hep-ph]].
- [71] T. Nomura and H. Okada, arXiv:2007.15459 [hep-ph].
- [72] H. Okada and M. Tanimoto, [arXiv:2005.00775 [hep-ph]].
- [73] H. Okada and M. Tanimoto, Phys. Rev. D **103** (2021) no.1, 015005 [arXiv:2009.14242 [hep-ph]].
- [74] K. I. Nagao and H. Okada, doi:10.1088/1475-7516/2021/05/063 [arXiv:2008.13686 [hep-ph]].
- [75] K. I. Nagao and H. Okada, [arXiv:2010.03348 [hep-ph]].
- [76] C. Y. Yao, X. G. Liu and G. J. Ding, Phys. Rev. D **103**, no.9, 095013 (2021) [arXiv:2011.03501 [hep-ph]].
- [77] X. Wang, B. Yu and S. Zhou, Phys. Rev. D **103** (2021) no.7, 076005 [arXiv:2010.10159 [hep-ph]].
- [78] M. Abbas, Phys. Atom. Nucl. **83** (2020) no.5, 764-769.
- [79] X. Du and F. Wang, JHEP **02**, 221 (2021) doi:10.1007/JHEP02(2021)221 [arXiv:2012.01397 [hep-ph]].
- [80] H. Okada and M. Tanimoto, JHEP **03** (2021), 010 [arXiv:2012.01688 [hep-ph]].
- [81] C. Y. Yao, J. N. Lu and G. J. Ding, [arXiv:2012.13390 [hep-ph]].

- [82] F. Feruglio, V. Gherardi, A. Romanino and A. Titov, JHEP **05**, 242 (2021) [arXiv:2101.08718 [hep-ph]].
- [83] S. F. King and Y. L. Zhou, JHEP **04** (2021), 291 [arXiv:2103.02633 [hep-ph]].
- [84] P. Chen, G. J. Ding and S. F. King, JHEP **04** (2021), 239 [arXiv:2101.12724 [hep-ph]].
- [85] T. Kobayashi, T. Shimomura and M. Tanimoto, [arXiv:2102.10425 [hep-ph]].
- [86] P. P. Novichkov, J. T. Penedo and S. T. Petcov, JHEP **04**, 206 (2021) [arXiv:2102.07488 [hep-ph]].
- [87] G. J. Ding, S. F. King and C. Y. Yao, [arXiv:2103.16311 [hep-ph]].
- [88] H. Kuranaga, H. Ohki and S. Uemura, [arXiv:2105.06237 [hep-ph]].
- [89] T. Kobayashi and S. Tamba, Phys. Rev. D **99** (2019) no.4, 046001 [arXiv:1811.11384 [hep-th]].
- [90] A. Baur, H. P. Nilles, A. Trautner and P. K. S. Vaudrevange, Phys. Lett. B **795** (2019) 7 [arXiv:1901.03251 [hep-th]].
- [91] T. Kobayashi, Y. Shimizu, K. Takagi, M. Tanimoto and T. H. Tatsuishi, Phys. Rev. D **100** (2019) no.11, 115045, Erratum: [Phys. Rev. D **101** (2020) no.3, 039904] [arXiv:1909.05139 [hep-ph]].
- [92] H. P. Nilles, S. Ramos-Sánchez and P. K. S. Vaudrevange, JHEP **02** (2020), 045 [arXiv:2001.01736 [hep-ph]].
- [93] H. P. Nilles, S. Ramos-Sánchez and P. K. S. Vaudrevange, Nucl. Phys. B **957** (2020), 115098 [arXiv:2004.05200 [hep-ph]].
- [94] S. Kikuchi, T. Kobayashi, S. Takada, T. H. Tatsuishi and H. Uchida, Phys. Rev. D **102** (2020) no.10, 105010 [arXiv:2005.12642 [hep-th]].
- [95] S. Kikuchi, T. Kobayashi, H. Otsuka, S. Takada and H. Uchida, JHEP **11** (2020), 101 [arXiv:2007.06188 [hep-th]].
- [96] K. Ishiguro, T. Kobayashi and H. Otsuka, [arXiv:2010.10782 [hep-th]].
- [97] G. J. Ding, F. Feruglio and X. G. Liu, JHEP **01** (2021), 037 [arXiv:2010.07952 [hep-th]].
- [98] K. Ishiguro, T. Kobayashi and H. Otsuka, JHEP **03** (2021), 161 [arXiv:2011.09154 [hep-ph]].
- [99] K. Hoshiya, S. Kikuchi, T. Kobayashi, Y. Ogawa and H. Uchida, PTEP **2021** (2021) no.3, 033B05 [arXiv:2012.00751 [hep-th]].
- [100] S. Kikuchi, T. Kobayashi and H. Uchida, [arXiv:2101.00826 [hep-th]].
- [101] G. J. Ding, F. Feruglio and X. G. Liu, [arXiv:2102.06716 [hep-ph]].
- [102] H. P. Nilles, S. Ramos-Sánchez and P. K. S. Vaudrevange, Phys. Lett. B **808** (2020), 135615 [arXiv:2006.03059 [hep-th]].

- [103] A. Baur, M. Kade, H. P. Nilles, S. Ramos-Sanchez and P. K. S. Vaudrevange, JHEP **02** (2021), 018 [arXiv:2008.07534 [hep-th]].
- [104] H. P. Nilles, S. Ramos-Sánchez and P. K. S. Vaudrevange, Nucl. Phys. B **966** (2021), 115367 [arXiv:2010.13798 [hep-th]].
- [105] A. Baur, M. Kade, H. P. Nilles, S. Ramos-Sanchez and P. K. S. Vaudrevange, Phys. Lett. B **816** (2021), 136176 [arXiv:2012.09586 [hep-th]].
- [106] A. Baur, M. Kade, H. P. Nilles, S. Ramos-Sánchez and P. K. S. Vaudrevange, [arXiv:2104.03981 [hep-th]].
- [107] G. Ecker, W. Grimus and W. Konetschny, Nucl. Phys. B **191** (1981), 465-492.
- [108] G. Ecker, W. Grimus and H. Neufeld, Nucl. Phys. B **247** (1984), 70-82.
- [109] G. Ecker, W. Grimus and H. Neufeld, J. Phys. A **20** (1987), L807.
- [110] H. Neufeld, W. Grimus and G. Ecker, Int. J. Mod. Phys. A **3** (1988), 603-616.
- [111] W. Grimus and M. N. Rebelo, Phys. Rept. **281** (1997), 239-308 [arXiv:hep-ph/9506272 [hep-ph]].
- [112] W. Grimus and L. Lavoura, Phys. Lett. B **579** (2004) 113. [hep-ph/0305309].
- [113] P. P. Novichkov, J. T. Penedo, S. T. Petcov and A. V. Titov, JHEP **1907** (2019) 165 [arXiv:1905.11970 [hep-ph]].
- [114] T. Kobayashi, Y. Shimizu, K. Takagi, M. Tanimoto, T. H. Tatsuishi and H. Uchida, Phys. Rev. D **101** (2020) no.5, 055046 [arXiv:1910.11553 [hep-ph]].
- [115] N. Aghanim *et al.* [Planck], Astron. Astrophys. **641** (2020), A6 [arXiv:1807.06209 [astro-ph.CO]].
- [116] M. Fukugita and T. Yanagida, Phys. Lett. B **174** (1986) 45.
- [117] V. A. Kuzmin, V. A. Rubakov and M. E. Shaposhnikov, Phys. Lett. B **155** (1985), 36
- [118] Z. Maki, M. Nakagawa and S. Sakata, Prog. Theor. Phys. **28** (1962) 870.
- [119] B. Pontecorvo, Sov. Phys. JETP **26** (1968) 984 [Zh. Eksp. Teor. Fiz. **53** (1967) 1717].
- [120] K. Abe *et al.* [T2K Collaboration], Nature **580** (2020) 339.
- [121] P. Adamson *et al.* [NOvA Collaboration], Phys. Rev. Lett. **118** (2017) no.23, 231801 [arXiv:1703.03328 [hep-ex]].
- [122] G. C. Branco, R. G. Felipe and F. R. Joaquim, Rev. Mod. Phys. **84** (2012) 515 [arXiv:1111.5332 [hep-ph]].
- [123] M. Holthausen, M. Lindner and M. A. Schmidt, JHEP **1304** (2013) 122 [arXiv:1211.6953 [hep-ph]].

- [124] M. C. Chen, M. Fallbacher, K. T. Mahanthappa, M. Ratz and A. Trautner, Nucl. Phys. B **883** (2014) 267 [arXiv:1402.0507 [hep-ph]].
- [125] F. Feruglio, C. Hagedorn and R. Ziegler, JHEP **07** (2013), 027 [arXiv:1211.5560 [hep-ph]].
- [126] S. Ferrara, D. Lust, A. D. Shapere and S. Theisen, Phys. Lett. B **225**, 363 (1989).
- [127] M. Chen, S. Ramos-Sánchez and M. Ratz, Phys. Lett. B **801** (2020), 135153 [arXiv:1909.06910 [hep-ph]].
- [128] R. C. Gunning, *Lectures on Modular Forms* (Princeton University Press, Princeton, NJ, 1962).
- [129] B. Schoeneberg, *Elliptic Modular Functions* (Springer-Verlag, 1974).
- [130] N. Koblitz, *Introduction to Elliptic Curves and Modular Forms* (Springer-Verlag, 1984).
- [131] S. Antusch and V. Maurer, JHEP **1311** (2013) 115 [arXiv:1306.6879 [hep-ph]].
- [132] F. Björkeröth, F. J. de Anda, I. de Medeiros Varzielas and S. F. King, JHEP **1506** (2015) 141 [arXiv:1503.03306 [hep-ph]].
- [133] I. Esteban, M. C. Gonzalez-Garcia, M. Maltoni, T. Schwetz and A. Zhou, JHEP **09** (2020), 178 [arXiv:2007.14792 [hep-ph]].
- [134] S. Vagnozzi, E. Giusarma, O. Mena, K. Freese, M. Gerbino, S. Ho and M. Lattanzi, Phys. Rev. D **96** (2017) no.12, 123503 [arXiv:1701.08172 [astro-ph.CO]].
- [135] S. Davidson and A. Ibarra, Phys. Lett. B **535** (2002), 25-32 [arXiv:hep-ph/0202239 [hep-ph]].
- [136] A. Pilaftsis and T. E. J. Underwood, Nucl. Phys. B **692** (2004), 303-345 [arXiv:hep-ph/0309342 [hep-ph]].
- [137] T. Asaka and T. Yoshida, JHEP **09** (2019), 089 [arXiv:1812.11323 [hep-ph]].
- [138] A. Abada, S. Davidson, F. X. Josse-Michaux, M. Losada and A. Riotto, JCAP **0604** (2006) 004 [hep-ph/0601083].
- [139] E. Nardi, Y. Nir, E. Roulet and J. Racker, JHEP **0601** (2006) 164 [hep-ph/0601084].
- [140] A. Abada, S. Davidson, A. Ibarra, F.-X. Josse-Michaux, M. Losada and A. Riotto, JHEP **0609** (2006) 010 [hep-ph/0605281].
- [141] S. Blanchet and P. Di Bari, JCAP **0703** (2007) 018 [hep-ph/0607330].
- [142] S. Pascoli, S. T. Petcov and A. Riotto, Phys. Rev. D **75** (2007) 083511 [hep-ph/0609125].
- [143] S. Pascoli, S. T. Petcov and A. Riotto, Nucl. Phys. B **774** (2007) 1 [hep-ph/0611338].
- [144] K. Moffat, S. Pascoli, S. T. Petcov and J. Turner, JHEP **1903** (2019) 034 [arXiv:1809.08251 [hep-ph]].
- [145] A. De Simone and A. Riotto, JCAP **0702** (2007) 005 [hep-ph/0611357].

- [146] M. Y. Khlopov and A. D. Linde, Phys. Lett. B **138** (1984), 265-268 doi:10.1016/0370-2693(84)91656-3
- [147] J. R. Ellis, J. E. Kim and D. V. Nanopoulos, Phys. Lett. B **145** (1984), 181-186 doi:10.1016/0370-2693(84)90334-4
- [148] C. Jarlskog, Phys. Rev. Lett. **55** (1985) 1039.
- [149] P. I. Krastev and S. T. Petcov, Phys. Lett. B **205** (1988) 84.
- [150] M. Plumacher, Ph.D. Thesis [hep-ph/9807557].
- [151] G. F. Giudice, A. Notari, M. Raidal, A. Riotto and A. Strumia, Nucl. Phys. B **685** (2004) 89 [hep-ph/0310123].